ASPECTS OF THE MICROWAVE INDUCED PLASMA AS AN ELEMENT SELECTIVE DETECTOR FOR SUPERCRITICAL FLUID CHROMATOGRAPHY AND SUPERCRITICAL FLUID EXTRACTION

by

Gerald Roger Ducatte

Dissertation submitted to the Faculty of the Virginia Polytechnic Institute and State University in partial fulfillment of the requirement for the degree of

Doctor of Philosophy

in

Chemistry

APPROVED:

Gary L. Long, Chairman

Mark R. Anderson

Joseph S. Merola

Harold M. McNair

Larry T. Taylor

December 1993

Blacksburg Virginia

ASPECTS OF THE MICROWAVE INDUCED PLASMA AS AN ELEMENT SELECTIVE DETECTOR FOR SUPERCRITICAL FLUID CHROMATOGRAPHY AND SUPERCRITICAL FLUID EXTRACTION

by

Gerald Roger Ducatte

Committee Chairman: Dr. Gary L. Long

Chemistry

(Abstract)

The introduction of supercritical CO_2 at packed column supercritical fluid chromatography (SFC) flow rates is shown to significantly affect the excitation characteristics of a helium microwave induced plasma (He MIP). In this work, the influence of CO_2 on specific atomic and ionic transitions of Cl, Br, I, P, and S is described. Also presented is the determined relationship between transition energy and degree of signal depression resulting from the introduction of CO_2 to the plasma. Attempts to enhance the emission signals of non-metals by introducing H_2 into a He MIP are discussed. The inadequacy of excitation temperature, ionization temperature, rotational temperature, and electron number density measurements to determine the effect of CO_2 on the excitation characteristics of a He MIP is also described. However, application of kinetic theory and a recently developed theory on charge transfer allows a reasonable series of mechanisms to be developed that describe the excitation processes of a He MIP to which supercritical CO_2 is added. The remainder of this work describes a direct interface between a supercritical fluid extraction (SFE) vessel and an Ar MIP for the purpose of element selective detection. The response of the plasma to the introduction of sample via SFE at a variety of extraction temperatures, pressures, and sample concentrations is presented.

ACKNOWLEDGMENTS

I would like to thank my lovely wife Laurenze for giving me confidence and encouragement when the tasks at hand seemed overwhelming. I am also very grateful for her extreme patience and understanding in dealing with the many hours that I had to devote to course work and research when we really needed to spend time together. Finally, I would like to thank her for giving me a wonderful baby girl . Chelsea Marie has brought a new light into our lives which, among other things, has helped me to work that much harder to be successful at achieving my degree.

I wish to thank my parents Beverley and Gerald R. Ducatte, Sr. for the emotional support they have given me not just during my graduate school carrier, but all of my life. They provided me with gentle pushes along the way and had enough confidence in me to know that I will always do my best. I also wish to thank them for being wonderful role models, for without them to look up to and learn from I may very well have not been equipped with the social skills that were so critical in achieving my many goals in life.

There are not many people who are blessed with a balance of intelligence, common sense, and compassion. Dr. Long is one of these rare individuals, and I would like to express my deep respect for this great man. I wish to sincerely thank him for the guidance he has given me on both a scientific and personal level. The respect, support, and confidence he has given me right from the start was critical in my development as a chemist and a person. I am grateful for that. The financial support is also greatly appreciated, as It supplied me with more time to spend on research.

Finally, I would like to thank those people who have been behind the scenes, yet have played an important role in many aspects of my graduate experiences. These people include the current and past plasmen (and women): Dr. Keith McCleary, "Doct" Ward Mavura, Edwin Lancaster, and Shannon Burcham. Other chemists who I wish to thank for

their emotional support, scientific advise, and for just being good friends through all the rough times (i.e. organic and P-chem core courses) are: Dr. Vince Remcho, Dr. Bob Klute, Dr. John Rimoldi, Dr. Tony Molinero, Mojee Babie-Cline, Joannie Chin, and Mark Lester. I would also like to express my gratitude to the women in the Davidson Hall main office: Angie Miller, Wanda Ritter, and Linda Sheppard for their desperately needed technical support.

TABLE OF CONTENTS

ABSTRACT ii

ACKNOWLEDGMENTS iii

LIST OF FIGURES viii

LIST OF TABLES x

CHAPTER 1 INTRODUCTION 1

CHAPTER 2 EXPERIMENTAL 19

- Reagents 19
- SFC/SFE Instrumentation 19
- Sample Introduction 21
- Operational Conditions 24
- Microwave Cavity 25
- Microwave Torch 28
- Optical System 28
- Data Collection 31

CHAPTER 3 DIAGNOSTIC MEASUREMENTS OF THE He MIP 33

- Excitation Temperature 35
- Electron Number Density 36
- Ionization Temperature 37

CHAPTER 4 THE EFFECT OF H_2 AND CO_2 ON NON-METAL EMISSION LINE INTENSITIES IN A He MIP 42

- RESULTS AND DISCUSSION 43
  - Effect of CO_2 and H_2 on Non-metal Emission Line Intensities 43
  - Chlorine 43
  - Bromine 44
  - Iodine 44
  - Sulfur 45
  - Phosphorus 46
  - Signal Depression and Total Transition Energy 46
  - Effect of CO_2 on Excitation Temperature 48
  - Effect of CO_2 on Ionization Temperature 49
  - Effect of H_2 on Excitation Temperature 52
  - Effect of H_2 on Ionization Temperature 54
  - Effect of Added Gases on Plasma Geometry 54

SUMMARY 58

CHAPTER 5 A COMPARATIVE STUDY OF DIAGNOSTIC MEASUREMENTS FOR DETERMINING THE EFFECT OF CO_2 ON A He MIP 60

RESULTS AND DISCUSSION 60
Excitation Temperature 60
Fe 61
He 61
Cl 66

Electron Number Density 66

Ionization Temperature 70
Cd 70
Ca 70

Rotational Temperature 70
OH 71
N_2^+ 74

Failure of LTE-Based Diagnostic Measurements 74
Excitation Temperature 77
Electron Number Density 77
Ionization Temperature 78
Rotational Temperature 79

Charge Transfer Theory 82

Depletion of He^+ - Kinetic Considerations 83

SUMMARY 86

CHAPTER 6 STUDIES ON SUPERCRITICAL FLUID EXTRACTION-MIP-AES 87

RESULTS AND DISCUSSION 87
Plasma Stability 87
Difficulties with the Interface 88
Effect of Extraction Pressure on System Performance 89
Effect of Extraction Temperatureon System Performance 91
Linearity of SFE-MIP 91
Repeatability 94

SUMMARY 94

CHAPTER 7 CONCLUSIONS 96

REFERENCES 100

VITA 104

LIST OF FIGURES

Figure 1. Microwave Induced Plasma Cavity 4

Figure 2. Glass "T" for SFC Introduction 20

Figure 3. Head Space Generator 22

Figure 4. Nebulizer/Spray Chamber 23

Figure 5. Cross-sectional of HEMIP and Torch 26

Figure 6. Conventional Quartz Dimensions 29

Figure 7. Schematic of SFC-MIP Set up 30

Figure 8. Plot of Transition Energy Vs. Signal Depression 50

Figure 9. Effect of CO_2 on Excitation Temperature 51

Figure 10. Effect of CO_2 on Ionization Temperature 53

Figure 11. Effect of H_2 on Excitation Temperature 55

Figure 12. Effect of H_2 on Ionization Temperature 56

Figure 13. Axial Scan of Cl Ion Line 57

Figure 14. Boltzmann Plot of He for T_{exc} 63

Figure 15. Boltzmann Plot of He/CO_2 for T_{exc} 64

Figure 16. Slope Comparison Plot of T_{exc} with He and He/CO_2 Plasmas 65

Figure 17. Boltzmann Plot of Cl for T_{exc} 67

Figure 18. Boltzmann Plot of Cl for T_{exc} He/CO_2 Plasma 68

Figure 19. Slope Comparison Plot of T_{exc} (Cl) with He and He/CO_2 Plasmas 69

Figure 20. Rotational Spectra of OH Band (He and He/CO_2 Plasmas) 73

Figure 21. Rotational Spectra of N_2^+ Band (He and He/CO_2 Plasmas) 75

Figure 22. Boltzmann Plot of N_2^+ for T_{rot} 80

Figure 23. Boltzmann Plot of OH for T_{rot} 81

Figure 24. Axial Scan of He^+ for He and He/CO_2 Plasmas 85

Figure 25. Analyte Deposit in Glass "T" used for SFE-MIP..... 90

Figure 26. Extractograms of Ferrocene..... 92

Figure 27. Peak Height vs. Concentration of Fe (SFE-MIP)..... 93

LIST OF TABLES

Table 1. Instrumentation 32

Table 2. Constants for Excitation Temperature Determinations using He..... 38

Table 3. Constants for Excitation Temperature Determinations using Fe..... 39

Table 4. Constants for Excitation Temperature Determinations using Cl..... 40

Table 5. Constants for Ionization Temperature Determinations using Ca & Cd..... 41

Table 6. Summary of Transition Energy vs. Signal Depression..... 47

Table 7. Comparison of Temperatures Obtained with Diagnostic Measurements... 62

Table 8. Constants for Rotational Temperature Determinations using OH..... 72

Table 9. Constants for Rotational Temperature Determinations using N_2^+..... 76

Chapter 1

INTRODUCTION

Purpose

The purpose of this work is to examine the technique of plasma emission spectrometry as an element specific detector for supercritical fluid chromatography (SFC) and supercritical fluid extraction (SFE). Specifically, a helium based microwave induced plasma is employed as a detector for non-metals with packed column SFC using CO_2 as the mobile phase, while an Ar-based plasma is used for detection of metals extracted from a solid matrix via SFE.

The introduction of SFC mobile phases into analytical plasmas is shown in this work and other studies to significantly affect the excitation properties of the discharge. A decrease in the ability of the He MIP to promote electronic transitions of the analyte in the presence of CO_2 has been commonly observed through the depression of emission signals of non-metal species [1-8], yet the true nature of this phenomena has not been reported in the literature. Therefore, a significant portion of this dissertation is devoted to an in-depth examination of the effect of supercritical CO_2 on the He MIP with respect to signal depression of non-metals, and correlating these observations with the results of diagnostic methods to determine the temperature of the plasmas. In an attempt to counteract the signal depressing effect of CO_2, another portion of this work examines the effect of H_2 on the He MIP. The addition of this gas has been shown to enhance atomic emission signals of certain elements present in a He discharge[9,10].

A logical extension of the use of the MIP as an element specific detector for SFC is the use of this technology for SFE, as supercritical CO_2 is the medium responsible for analyte transport in both systems. The response of a microwave induced plasma to the introduction of supercritical CO_2 via a SFE system has not yet been reported in the

literature. Studies in this area could provide information leading to the development of an analytical technique which is capable of direct detection of extracted analytes without incorporating a time consuming intermediate chromatographic step. Initial studies on SFE-MIP are presented in this dissertation in order to demonstrate the feasibility of this technique for element specific detection of analytes extracted with supercritical CO_2.

To properly place this work into context, the remainder of this chapter will be concerned with the historical aspects of the MIP, plasma support gases, supercritical fluid chromatography and extraction, conventional and plasma based detectors, line selection criteria, and mechanisms for analyte excitation.

HISTORICAL

Atomic emission spectroscopy [AES] is a powerful method of chemical analysis. Current spectroscopic systems employing a variety of emission sources provide for qualitative and quantitative determinations of nearly 70% of the elements contained in the periodic table [11]. While most of the atomic emission analyses carried out today involve determination of the total concentration of a particular element present in a sample, AES can also serve as a method of element selective detection for chromatography. The latter arrangement affords identification and quantitation of compounds as they elute from the analytical column of a variety of chromatographic systems.

Microwave-Induced Plasmas with the Beenakker Cavity

The advent of the Beenakker TM_{010} resonant frequency microwave cavity in 1976 [12] provided a means by which atomic emission spectroscopy could be performed with atmospheric pressure microwave induced plasmas (MIP) utilizing both Ar and He. A modified version of this cavity, as described below, was employed for the studies described in this dissertation. While the unmodified Beenakker cavity design provided benefits over

other cavities such as enhanced sensitivity and the option of viewing the plasma in an axial mode, it did suffer from inefficient power transfer from the microwave generator. Its fixed loop configuration, which relies upon the use of external resistive loads to achieve an impedance of 50 ohm, made the tuning of the cavity inefficient and cumbersome. Additionally, effective operation of the TM_{010} was limited to <50W, as the loop did not provide a sufficiently high coupling coefficient to obtain matching at higher power levels. Plasmas generated at these relatively low forward powers are limited in available excitation energy.

In an attempt to overcome the problems and limitations experienced with the TM_{010} cavity Boss *et al.* [13] modified the original design by incorporating a movable capacitively coupled antenna probe. This device afforded a more efficient and easier method of impedance matching between the microwave generator and the resonant cavity. This alteration also allowed for more energetic plasmas to be sustained, as they could now be operated at much higher microwave powers. The probe could simply be translated along the radial face of the cavity to the position which yielded a match between the impedance of the two electrical systems. This match is required in order achieve a state of critical coupling which results in the cavity being supplied with maximum forward power and, consequently, minimum reflected power. This minimization of reflected power plays an important role in extending the lifetime of the magnetron generator. The work of Boss *et al.* has been noted to be the most significant modification of the original TM_{010} [14] because it provided; 1) greater than 90% coupling efficiency, 2) operation at 20% lower power than the original design, and 3) analytically useful He or Ar plasmas at applied powers of over 150 W. This modified cavity design (Figure 1) has been evaluated and utilized in many studies performed by Long *et al.* [2,8,15,16]. These previous reports have involved introduction of both nebulized aqueous samples and chromatographic effluent

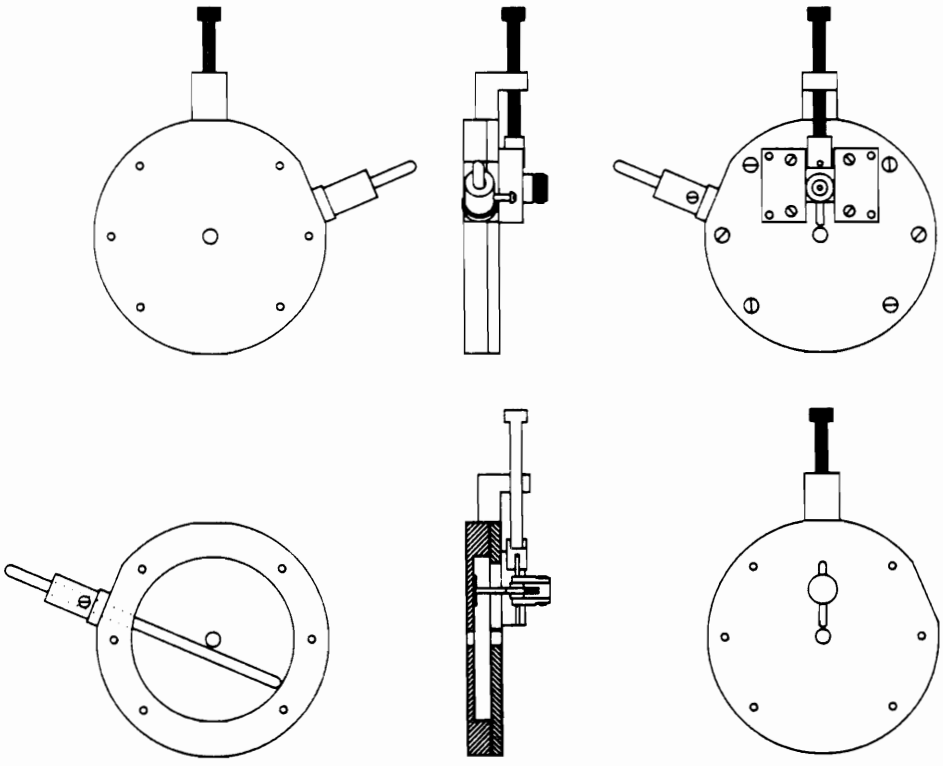

Figure 1: Modified Beenakker Cavity

(Adapted from reference 38)

with SFC. This design is also used in the current investigations.

Argon vs Helium - Based Plasmas

Since the early stages of development of microwave induced plasmas two plasma gases have proven to be the most useful for analytical determinations; helium and argon. Because each of these gases is utilized in the separate studies described in this dissertation it is necessary to highlight the major differences in the analytical properties of these plasma gases. The relatively low ionization potential of the argon atom, 15.8 eV, provides for ease of operation of a wide variety of plasma types (i.e. ICP, MIP, glow discharge, etc.). It is for this reason that initial plasma studies were conducted using Ar as the main plasma gas. Ar-based analytical plasmas have been successful in many analytical applications, including systems which involve direct aqueous introduction or element selective detection chromatography. However, the utility of the Ar MIP is limited mainly to excitation of metal species. Because most metals require less than 10.5 eV to remove one electron from the atom, the Ar plasma is of sufficient energy to promote a majority of atomic transitions and some ionic transitions. Analyses of non-metals is much more demanding, as many transitions require on the order of 35 eV to achieve adequate population densities of ionic electronic states. The Ar plasma species simply do not possess enough energy to promote many nonmetal transitions.

As more efficient non-metal plasma emission detection systems were being pursued, the attention of many researchers quickly turned to alternate plasma gases in hopes of achieving a more energetic plasma, and ultimately the promotion of the high energy non-metal transitions. It was during this stage of development that the analytical utility of the He MIP was realized. The ionization potential of He is 24.5 eV, nearly 1.5 times that of Ar. This difference in ionization energy of the gases results in an analytical plasma that is more difficult to achieve and maintain relative to the Ar plasma, as the applied power required to

sustain a controlled plasma is increased with He. Additionally, a significant increase in flow rate of plasma gas is required to operate the He discharge, and an increased sensitivity to minor fluctuations in tuning efficiency of the system, relative to argon, is evident for the He plasma. Critical coupling of the He MIP system is therefore more difficult to achieve than with Ar-based systems. Even with the minor difficulties in operation of the MIP, the ability of He to efficiently excite nonmetal transitions significantly outweighs any tuning or matching problems. It is interesting to note that while many microwave plasma sources have been easily adapted to accommodate helium plasmas for the purpose of emission detection of non-metals, the ICP, with its basic discharge tube configuration and inherently large power (kilowatt) requirements, has displayed limited success with pure He discharges. This fact is mentioned as it provides a distinction between the MIP and ICP with respect to the detection of non-metal species.

Although the Ar MIP is limited in excitation energy, it was selected for the SFE-MIP studies described in Chapter 6 for the reason of its ease of use relative to He, and a metal species was being determined. On the other hand, the SFC investigations described in Chapters 4 and 5 are centered around the effect of CO_2 on non-metal species. These studies required the use of the more energetic He MIP.

Supercritical Fluid Chromatography

A supercritical fluid can be defined as a substance that has been elevated to its critical temperature and pressure such that it is no longer a liquid or gas but is in fact a fluid in a supercritical state. Since the concept of utilizing a supercritical fluid as a mobile phase for chromatography by Lovelock in 1958, many investigations employing supercritical fluid chromatography (SFC) have been carried out. The first study was performed by Klesper in 1961 with the separation of porphyrins [17]. Although SFC has existed for over 30 years, it has only been within the last decade that the analytical utility of SFC has been moderately

explored and realized. The somewhat unique characteristics of a supercritical fluid as a mobile phase, relative to a liquid or gas, provides for certain chromatographic advantages over either gas chromatography (GC) or liquid chromatography (LC). The combination of physical properties of a supercritical fluid, which may be thought of as a hybrid of a liquid and a gas, presents an efficient compromise between solvating strength and molecular diffusivity. The main advantage of SFC over GC is in versatility. In GC, the mobile phase simply provides a means by which sample is transferred through the column, and generally no chemical interactions occurr between mobile phase and analyte. This technique relies on relatively high column temperatures to effectively partition the analyte into the mobile phase. Thus, GC is limited to analysis of approximately 15% of all known compounds; those which are both thermally stable and volatile. On the other hand, with proper selection of mobile phase composition, SFC has been successfully applied to many thermolabile and nonvolatile compounds, including moderate molecular weight polymers. With respect to LC, SFC has the distinct advantage of being compatible with a larger variety of detectors. While a majority of analytes separated by LC are limited to ultra-violet (UV) or refractive index (R) detection, analytes separated by SFC are able to be detected with most of the LC-type detectors and, more importantly, with most GC-like detectors. The wide range of detectors compatable with SFC allows for efficient detection of many analyte types without sacrificing sensitivity.

Because the studies presented in this dissertation deal strictly with the use of supercritical carbon dioxide as the SFC mobile phase, the basis of this focus must be briefly discussed and justified. CO_2 possesses certain physical and chemical characteristics which have ultimately made it the most popular mobile phase for SFC. Before the development of commercially available SFC systems, minor modifications of standard HPLC instrumentation were sufficient to achieve the relatively low supercritical conditions of CO_2: critical pressure = 72.9 atm, and critical temperature = 31.3°C. These easily achieved

supercritical conditions had a significant impact on the selection of CO_2 as the mobile phase in initial SFC studies. In addition to the low critical parameters of CO_2, this gas is non-toxic, non-flammable, and generates no hazardous waste. It is also compatible with a variety of conventional LC and, because of the gaseous nature of CO_2 at ambient conditions, GC detectors without the requirement of solvent elimination. As a mobile phase, supercritical CO_2 is capable of dissolving many non polar compounds in addition to some compounds of moderate polarity with the employment of density programming. The addition of relatively small percentages (2-10 %) of polar "modifiers" such as methanol has extended the utility of CO_2 to more moderately polar compounds and some highly polar species. While some polar modifiers have been shown to effect the response of certain detectors, binary CO_2/modifier mobile phases still provide an adequate alternative to highly polar, and somewhat destructive, supercritical fluids such as NH_3 for analysis of more polar samples.

Supercritical Fluid Chromatography - Conventional Detectors

Quantitative detection of analytes in supercritical fluids has been demonstrated with a variety of both universal and specific detectors. The four major detectors that have been utilized for SFC are the flame ionization detector (FID), ultraviolet absorption (UV) spectrometer, mass spectrometer (MS), and fourier transform infrared spectrometer (FTIR). The main driving force behind the development of the MIP as a detector for SFC is the absence of a detector which is completely compatible with the many modes of SFC. It is not the intent of this author to lessen the credibility of conventional detectors, as each provide for efficient analysis of many compounds separated by SFC. Instead, the following paragraphs highlight some of the incompatibilities of SFC with the aforementioned conventional detection methods.

While the conventional GC-compatible FID has been modified to accommodate supercritical fluids at flow rates typical of packed column SFC and is capable of low nanogram detection limits of certain compounds, its universal response to organic compounds does not allow accurate detection of coeluting species. In this instance, quantitative detection of analytes becomes critically dependent on the degree of chromatographic resolution. Additionally, the use of polar modifiers is extremely limited with SFC-FID because of background interferences generated by these organic molecules [20]. Multi and fixed wavelength UV absorbance detectors have also been made compatible with both capillary column and packed column SFC. Picogram detection limits of specific compounds have been reported with SFC-UV [21,22]. However, while CO_2 exhibits little background absorbance in the 200-800 nm region, the addition of modifiers, which are vital in achieving many SFC separations, have been shown to change the background dramatically. Another, more obvious, limitation of SFC-UV is that the analyte must contain or allow attachment of a chromaphor. This condition severely limits the utility of this technique. On-line detection of chromatographic effluent with FTIR has proved to be a useful technique for analyses of many IR-active compounds. As with UV absorption spectroscopy, the addition of even small amounts of organic modifiers obscure wide regions of the observed spectrum. CO_2 absorbs strongly in the 3600-3400, 2500-2200, and 750-600 cm^{-1} regions and decreases the transmission in several other regions with increased mobile phase density. Thus, it has been necessary to develop SFC-FTIR interfaces which eliminate the solvent prior to analyte detection [23,24]. Of the two major mass spectrometric ionization methods, chemical ionization (CI) and electron impact (EI), CI has shown a higher degree of compatibility with SFC with respect to decompressed CO_2. Even with large partial pressures of CO_2 being present in the CI ion source, the sensitivity of the system is not significantly changed. This is thought to be due to the low proton affinity of CO_2. However, EI, which generates a larger degree of fragmentation and provides the more

detailed information required in many analyses, does suffer from some incompatibilities with the rapidly decompressing CO_2. The formation of CO_2 clusters at the outlet of the SFC restrictor is thought to cause incomplete desolvation of the analyte molecules before their impact with the electrons in the ion source. This phenomena severely limits the attainable detection limits of EI/SFC/MS. An additional difficulty with SFC-MS arises within the mass analyzer. Sector mass spectrometers, which require higher vacuum relative to quadrapole units, are not able to adequately sample the CO_2 stream as a result of the high pressure conditions of SFC.

Thus, limitations in the applicability of each of these conventional detection systems with analyses employing various SFC mobile phases, modes, and/or different sample types has left room for the development of analytical plasmas as detectors for SFC.

Supercritical Fluid Chromatography-Microwave Induced Plasma

SFC-MIP has been successfully performed with a variety of microwave cavity structures, the most popular of which include the surfatron, microwave plasma torch (MPT), and the Beenakker TM_{010} resonant cavity. This analytical technique has received much attention over the past 5 years. Spectrometric detection of analytes in supercritical fluids with analytical plasmas has demonstrated much success with both capillary and microbore packed column SFC [1-8, 15, 25-28]. Volumetric flow rates of supercritical fluids in open tubular columns is on the order of .001 - .01 mL/min, depending on the dimensions of the column. Microbore packed SFC flows are typically on the order of 1mL/min. This relatively large difference in volumetric flow rates between the two modes of chromatography readily distinguishes the applicability of the plasma source. While the MPT and surfatron devices are capable of analyte detection with the lower flow rates associated with capillary column SFC, these cavity designs generate plasmas which become unstable or even extinguished with the introduction of SFC mobile phase at packed column

flow rates. The Beenakker TM_{010} cavity is the only design to date which is capable of generating an analytically useful plasma when coupled with microbore packed column SFC.

The introduction of SFC mobile phase to low-powered microwave induced plasmas has been shown to significantly effect certain characteristics of both the Ar and He MIPs [2]. With this perturbation, the efficiency of the plasma at promoting electronic transitions, particularly those of non-metals, is hindered. The redistribution, or "loss", of plasma energy results in a decrease in sensitivity of the system toward certain elements at specific emission wavelengths. This phenomena has been reported in the literature by a number of research groups utilizing either MIP or ICP detection systems for SFC[1-8]. Several theories have emerged in an attempt to explain the altering of plasma properties resulting from the introduction of SFC mobile phase. One theory suggests that plasma energy is depleted with the introduction of molecular gases such as CO_2 or N_2O, as a significant portion of energy goes into the dissociation of these species [29]. With this reduction of energy, the plasma no longer possesses sufficient energy to efficiently populate excited state levels of many elements of interest. Subsequently, the measured emission intensities are decreased. A second theory, termed charge transfer, argues that the decrease in plasma energy is due to the decrease in population of the plasma species which is responsible for a majority of non-metal analyte excitation. The latter theory will be discussed in detail in subsequent paragraphs as it pertains directly to results observed in the current studies.

The effect of supercritical CO_2 on the excitation properties of an Ar MIP has been demonstrated [15]. Measurement of the electron number density and excitation temperature of an Ar MIP with and without the addition CO_2 reveals a decrease in the excitation energy of this low powered plasma in the presence of this added gas. Introduction of ~ 0.3% CO_2, as related to total gas entering the plasma torch, resulted in a decrease in n_e^- by an order of magnitude. This finding suggests that the number of free electrons and, subsequently, the number of Ar ionic species in the plasma is deminished with the introduction of CO_2. The

T_{exc} of the Ar MIP was also shown to decrease in the presence of CO_2. In this case, 10 mL/min of added CO_2 resulted in a 30% reduction in T_{exc}. Two important conclusions can be drawn from this investigation: 1) the introduction of supercritical CO_2 significantly decreases the excitation energy of the Ar MIP. 2) the electron number density and excitation temperature measurements prove to be adequate diagnostic methods in evaluating the energy of the Ar MIP. These considerations become important in Chapters 4 and 5 of this dissertation, as the applicability of these and other diagnostic methods for evaluating a He MIP is determined

Line Selection in SFC-MIP

The element selective nature of plasma atomic emission detection has shown its advantages in detection of analytes that cannot be easily resolved chromatographically from the solvent or another component of a mixture. In this way, MIP detection of chromatographic effluent is able to tolerate peak overlap due to coeluting species. However, spectral overlap of the wavelength of interest with that of the mobile phase, in certain instances, does require that extra care be taken in the selection of emission lines. When SFC-MIP analyses employ either N_2O or, more commonly, CO_2 as the mobile phase, the generation of dissociation products of these molecules in the plasma does not afford an infinite spectral window of the UV-visible-or IR electromagnetic spectral regions. Each of these dissociation species gives rise to potentially interfering emission bands. However, employment of these mobile phases does allow for interference free detection of metals and nonmetals in large portions of these commonly observed spectral regions. Carnahan and Hieftje have demonstrated the advantages of observing non-metal emission lines in the IR relative to the UV or visible regions of the spectrum for SFC-MIP analyses [4, 6, 27, 28]. In the aforementioned study the background emission resulting from the introduction of N_2O

or CO_2 was closely examined in order to select the mobile phase which did not yield emission and interfere with observation of the analyte emission. In addition to spectral background interferences, the loss of analyte signal, mentioned earlier, plays a major factor in line selection of SFC-MIP analyses. If all excited energy levels for a given element were affected to the same degree by the introduction of SFC mobile phase, no additional line selection factor would enter an analyses. However, it has been shown that this is not the case. Carnahan *et al.* have noted that the intensity of emission occurring from the 912.2 nm Cl line was depressed to a lesser degree than the higher energy ionic 479.5 nm line with the introduction of either CO_2 or N_2O. This phenomena presents an additional consideration in line selection for SFC-MIP. Selection of emission lines based upon relative intensity alone is not adequate when supercritical fluids enter the plasma. Knowledge of the effect of the various SFC mobile phases on particular elements and their electronic transitions presents the need for a more detailed understanding of the relationship between signal depression and transition energy. Chapter 4 in this dissertation describes this effort to elucidate such relationships.

Analyte Excitation in He Microwave Induced Plasmas

In an attempt to understand the depression of emission signals observed in a He MIP with the introduction of SFC mobile phase, which is a major objective of these dissertation studies, it is necessary to consider the chemical and physical processes that occur in the He plasma. Specifically, it is important to have knowledge of the plasma species and reaction mechanisms which are responsible for excitation of the analyte species. Many reaction schemes have been postulated since the early 1970s which attempt to describe the process of electronic excitation of elements present in analytical plasmas. Some of these postulated mechanisms attempted to describe the events which were thought to occur in one general plasma type (ie. Ar or He). Because it is thought that similar

processes occur in the ICP and the MIP, the theories developed for the Ar ICP have been readily applied to the MIP. The investigations described in Chapters 4 and 5 of this dissertation deal with helium MIPs. Therefore, we will consider only those processes which are thought to play a role in the excitation of analytes in He plasmas.

In 1977 Beenakker [12] evaluated the performance of an atmospheric pressure MIP generated with the TM_{010} cavity for element selective detection of gas chromatographic effluent. In this study the excitation processes thought to be responsible for the observed electronic transitions of a variety of nonmetals were considered. Reaction mechanisms between the analyte and the He metastable, atomic ion, and molecular ion were postulated. Additionally, the role of the free electron in analyte excitation was considered. The likelihood of energy exchange between the analyte and certain plasma species due to elementary particle collisions served as the basis of possible direct or recombination excitation mechanisms. A conclusion of this study was that the role of Penning ionization (reaction 1) and the metastable He species seemed to provide a logical reaction scheme for the excitation of a majority of the elements studied.

$$He^m + X \text{ ----> } He + X^+ + e^- \qquad (1)$$

Here, He^m represents the helium metastable, e^- is the free electron, and X represents the analyte. It is interesting to note that this study also concluded that the role of He^+ species in analyte excitation was minimal, as no evidence supported any related mechanism [12]. Subsequent investigations [30,31] attempted to describe possible non-metal excitation mechanisms taking into consideration not only the energy exchange between colliding species but the relative populations of plasma species as well as their relative lifetimes. Particular attention was paid to the role of the metastable He atom and molecule due to the relatively long lifetimes (1-10 μs) at atmospheric pressure [32-35], and the atomic and

molecular ions, due to their combined populations being approximately 10^{15}/cc. Mechanisms thought to be responsible for the electronic excitation of observed emission of Cl, Br, I, P, and S as determined by Skogerboe [30] were limited to three general collisional schemes: simultaneous ionization and excitation between atomic and molecular He ions and the nonmetal (reactions 2, 3), sequential ionization and excitation in a two step process involving atomic and molecular He metastable species (reactions 4-9), and double ionization, by collision with either metastable species, followed by electron-ion radiative recombination (reaction 10).

Simultaneous:

$$He^+ + X \rightarrow He + X^{+*} \quad (2)$$

$$He_2^+ + X \rightarrow 2He + X^{+*} \quad (3)$$

Ionization:

$$He^m + X \longrightarrow He + X^+ + e^- \quad (4)$$

$$He_2^m + X \rightarrow 2He + X^+ + e^- \quad (5)$$

$$e^- + X \rightarrow e^- + X^+ + e^- \quad (6)$$

Excitation:

$$He^m + X^+ \longrightarrow He + X^{+*} \quad (7)$$

$$He_2^m + X^+ \rightarrow 2He + X^{+*} \quad (8)$$

$$e^- + X^+ \rightarrow e^- + X^{+*} \quad (9)$$

Recombination:
Reactions 4-6 followed by:

$$X^{2+} + e^- \rightarrow X^{+*} \quad (10)$$

Here, the term $^{+*}$ denotes the excited ion. Each of these reaction schemes seemed to provide logical pathways to the population of specific nonmetal energy states which result in significant emission at certain wavelengths. Recent studies performed by Carnahan have revealed evidence of the influence of the population of He^+ species in nonmetal analyte excitation in He atmospheric MIPs [45, 46]. Detailed attention will be given to these studies in Chapter 5 as they play an important role in explaining the events observed in the current investigations.

Plasma Diagnostic Measurements

In attempting to understand the processes taking place in a He MIP with the introduction of CO_2, it is not enough to only look at the previously described mechanisms of analyte excitation. It is also necessary to consider the amount of energy contained in a He plasma under different conditions, via diagnostic methods. Historical aspects of the plasma diagnostic measurements utilized in these studies are presented in the subsequent paragraphs.

While reduced pressure He plasmas have relied heavily on electrical probes for diagnostic measurements [30], such devices do not allow accurate diagnostic measurements to be performed on atmospheric pressure plasmas. Instead, measurement of the relative intensity of certain spectrometric species and knowledge of the appropriate spectrometric constants allows for the determination of a variety of plasma conditions. Spectrometric measurements such as excitation temperature (T_{exc}), electron number density (n_{e^-}), ionization temperature (T_{ion}), and rotational temperature (T_{rot}) have been utilized to evaluate the excitation properties of a variety of analytical plasmas. These measurements have been useful at providing comparisons between different plasma types and between plasmas operated under various physical conditions. While many applications of these

diagnostic measurements seem to accurately describe the condition of plasmas, the existence of a state of thermodynamic equilibrium (TE) or, more specifically, local thermodynamic equilibrium (LTE) has been a topic of much controversy.

In order for a plasma to be considered in a state of LTE, the velocity distribution of all species must obey Maxwell relations, the relative population densities of excited atomic and ionic states within the same system must follow Saha distributions, and the relative population densities of atomic excited states of the same element must locally obey Boltzmann equilibria. With these requirements being met, calculations of plasma temperatures based upon LTE may be performed from spectrometric data.

It will be demonstrated in subsequent chapters that while the relationship between signal depression and transition energy for a variety of nonmetals in the He/CO_2 MIP has been revealed as a result of these studies, the cause of this phenomena cannot be determined by application of the most commonly employed LTE-based diagnostic measurements. Instead, the incorporation of a recently postulated charge transfer theory along with kinetic studies is used to provide a further understanding of the processes involved with analyte excitation in He MIPs.

Supercritical Fluid Extraction

The analytical utility of supercritical fluids for extraction of anaytes from a variety of matrices has been realized with the last 8 years. One characteristic of SFE which has played a large role in the promotion of this technique is the significant time advantage of this method over conventional extractions. Many Soxhlet extractions which normally require hours or even days to perform can be done in less than 30 minutes with SFE [18]. Additionally, the compatibility of the decompressed supercritical fluid, which is essentially a gas, with the sample requirements of GC analytes has made SFE-GC a viable on-line and off-line method of analysis. An even higher degree of compatibility exists between SFE

and SFC. Thus, the success of this technique has also helped to support the development of SFE, as SFE-SFC has demonstrated qualitative and quantitative chemical analyses with a host of analytes contained in biological, environmental, polymer, and other matrices [18]. However, while SFE-chromatography has proved a viable analytical technique for many types of analyses, the chromatographic step can take up to or greater than 30 minutes, depending on the method of separation, target analyte, and required resolution [19]. In some instances, elimination of the chromatographic step via direct analyte detection could provide a significant time advantage in the analysis of supercritical fluid extracts.

Chapter 6 of this dissertation will present results achieved with a novel interface which allows direct element selective detection of extracted analytes via SFE-MIP. Because this particular study deals with analysis of metals, Ar is used as the plasma gas instead of He. The operational parameters required for the complete dynamic-mode extraction of ferrocene from spiked sea sand are described. The response of the atmospheric pressure Ar MIP to the introduction of CO_2 at a range of extraction pressures is presented. The difficulties encountered with this technique with respect to analyte deposition prior to detection are also reported. While the initial studies presented in this section have been carried out with an unoptimized SFE-MIP system, monitoring of the atomic emission of Fe in the ferrocene extract with an Ar MIP reveals the potential of spectroscopic detection of analytes in supercritical fluid extract in the absence of a chromatographic step.

Chapter 2

EXPERIMENTAL

Reagents

Supercritical fluid chromatography grade CO_2 was purchased from Scott Specialty Gases (Plumsteadville, PA) with 1500 psi He headspace and a dip tube. Analytical -grade He, Ar, and H_2 were purchased from Airco (Murray Hill, NJ). 1-Bromopropane, triethyl phosphate, carbon disulfide, and diiodomethane were purchased from Aldrich Chemical Co. (Milwaukee, MI). HPLC-grade chloroform and methylene chloride were purchased from J. T. Baker Inc. (Phillipsburg,NJ). Aqueous Stock solutions of 1000 ppm of Fe and Cd were prepared in the laboratory according to standard procedures [36].

SFC / SFE Instrumentation

The CO_2 was prefiltered through a 0.5 μm stainless steel frit located in-line between the gas cylinder and the Suprex SFC/200A syringe pump. In order to simulate SFC-MIP conditions with respect to the introduction of CO_2, a 25 μm linear pressure restrictor was inserted into the side arm of a glass "T" (Figure 2). The "T" connector was mated to the side arm of the plasma torch through the use of a ball joint. This configuration, which orients the He and CO_2 flows orthogonal to each other, has been found to provide several advantages over central effluent introduction [16]. The glass "T" incorporated in these studies is a modified version of the design utilized by Motley and Long [16]. The inner diameter of the glass arm into which the SFC restrictor is inserted has been reduced from 5 mm to 500 μm. This new design provides a decrease in He back pressure on the septum, thereby eliminating inadvertent separation of the septum from the union during the chromatographic run. Additionally, this modification affords a greater stability of the restrictor (~ 300 μm o.d.) as the smaller hole provides for a more snug fit.

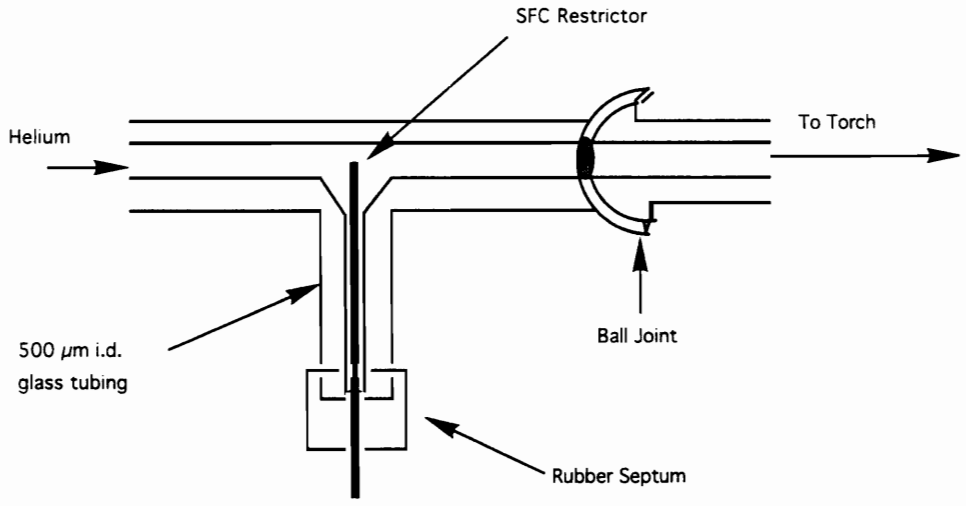

Figure 2: Glass "T" used For Introduction of SFC Mobile Phase to the MIP

A 1 mm X 15 cm Deltabond phenyl column packed with 5 μm particles was employed to simulate microbore SFC flow rates. The extraction vessel used in this study was a 1.67 mL stainless steel cell (Keystone Scientific). Spiking of the sea sand was achieved with either a 1000 μL Eppindorf ® micropipet of a 0.25 mL hypodermic syringe. After dispensing the analyte and solvent into the half-full cell, the end of the cell was replaced and the unit was placed in the oven at 50°C to evaporate the methylene chloride. Then the extraction cell was packed as full as possible with the remaining pre-extracted sand (total weight of sand ~ 1.3 g) to reduce dead volume, and was heated in the oven to achieve the critical temperature of CO_2.

Sample Introduction

Non-metal samples were introduced into the plasma as organic vapor with the use of a headspace generator (Figure 3). Operation of this laboratory constructed apparatus involved placing 10-30 mL of organic sample in the flask portion of the generator and opening the 3 glass valves to allow the main He flow to sweep the sample vapor into the plasma. Reproducible sample introduction was achieved by opening all 3 valves to full-flow position and setting the He flow with the rotameter upstream of the headspace generator. This constant supply of analyte was necessary to perform the wavelength scans of the non-metal emissions.

The thermometric species used in the temperature measurements were introduced into the plasma as aqueous solutions which were prepared by standard procedures [16]. Introduction of these aqueous samples required the use of a pneumatic nebulizer, Scott spray chamber, and peristaltic pump for generation of an analytically useful sample aerosol. With the help of the auxiliary He flow, the resulting aerosol was directed into the side arm of the plasma torch. A diagram of this sample introduction system is shown in Figure 4.

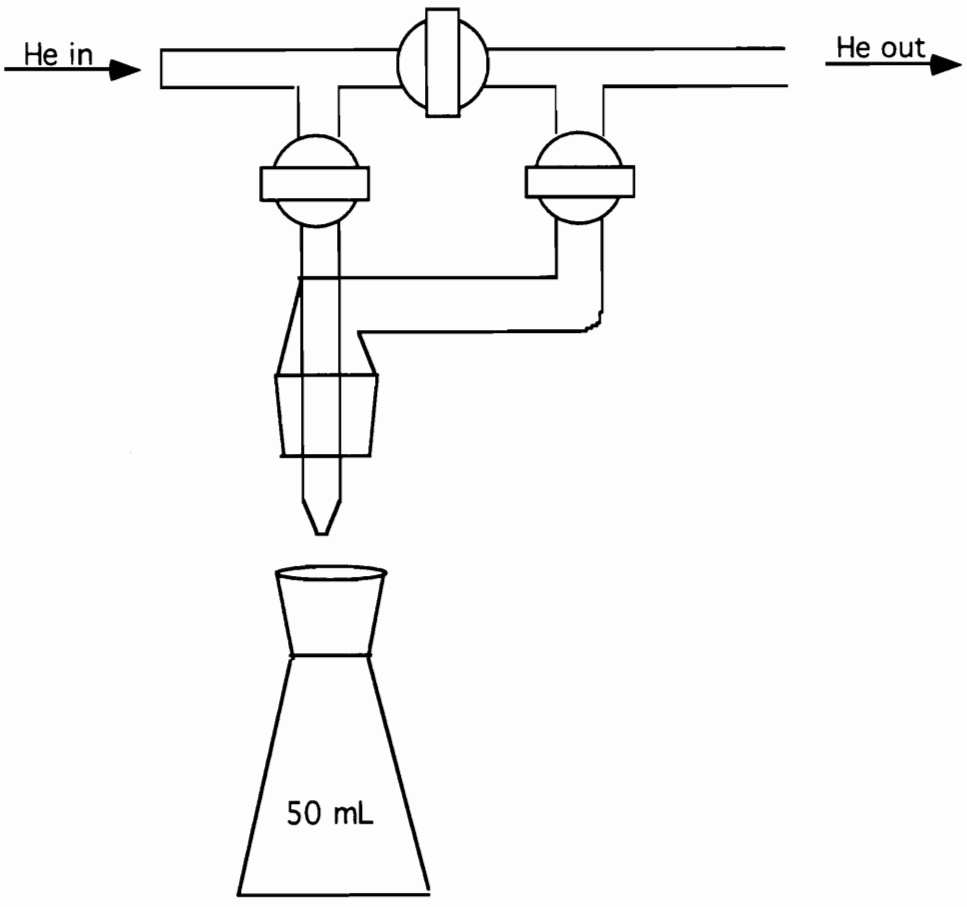

Figure 3: Headspace Generator used for Introduction of Organic Sample Vapor to the MIP

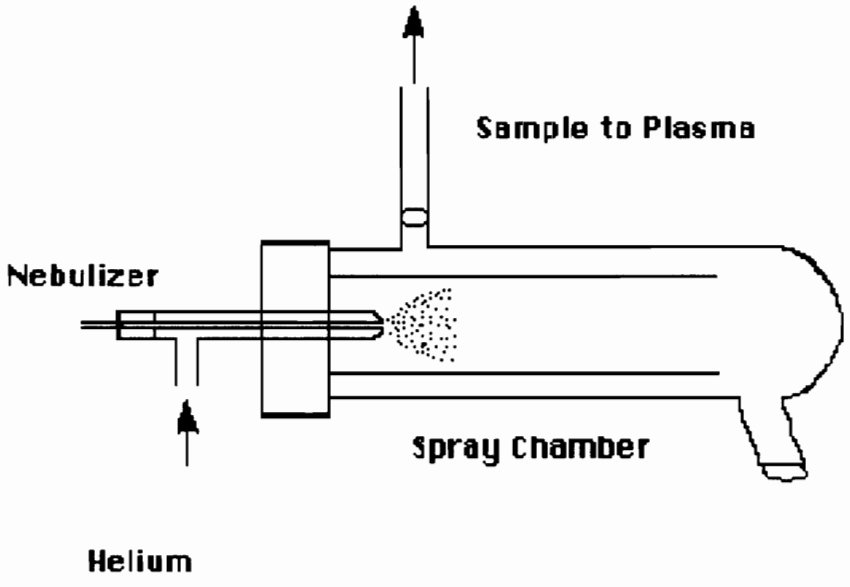

Figure 4: Meinhard Nebulizer and Scott Spray Chamber used for Aqueous Sample Introduction to the MIP

Introduction of the extracted samples was achieved with a length of either 25 or 50 μm i.d. fused silica capillary tubing (Scientific Glass Engineering, Austin TX) which served to transport the supercritical fluid extract from the outlet of the extraction cell to the plasma. The SFC oven was placed close to the plasma cavity in order to minimize the length of unheated restrictor, thus minimizing the chances of analyte deposition inside the restrictor.

Operational Conditions

The plasmas described in Chapter 4 were sustained with a He main gas flow of 3L/min. This flow was directed through the headspace generator as described above. The excessive amount of organic sample vapor entering the He discharge often resulted in an unstable plasma. It was therefore necessary to introduce an auxiliary He flow of 3.5 L/min in order to achieve and maintain a stable, centered plasma. The secondary He flow was introduced through a glass connector located physically between the headspace generator and the "T" used for the H_2 introduction. The hydrogen flows employed in this investigation were 100 and 500 mL/min, which represent 1.5 and 7.5 % , respectively, of the total gas flow entering the discharge tube. The pressure of CO_2 maintained throughout the chromatographic system was set at 100 atm. This pressure resulted in a decompressed flow rate, as measured at the outlet of the SFC restrictor, of approximately 25 mL/min entering the plasma torch.

The microwave generator was operated at a range of 150 - 300 W forward power for measurement of the diagnostic parameters. 150W was selected as the lower limit based upon the results obtained by Motley and Long[2]. Operation of a He plasma in the latter study from 140-200W revealed that maximum S/N ratio for element selective detection of sulfur is achieved at 150 W for this nonmetal. The upper limit represents an operating power which has been successfully applied to "moderate-power" analytical plasmas and which, in our system, results in the maximum amount of tolerated reflected microwave

power. Application of higher applied powers in this setup significantly decreases the lifetime of the magnetron generator. An applied power of 150W was selected for the nonmetal emission measurements as this level yields maximum S/N and provides for a more stable He discharge relative to plasmas operating at higher forward powers. The reflected microwave power was redirected with a power circulator into a power meter which allowed accurate monitoring of the power reflected back from the cavity. Reflected power values of <1W were found for the studies performed at 150W, and < 4W at higher applied powers.

The plasmas utilized for the studies described in Chapter 5 were sustained with a total He flow of 5L/min. Approximately 3L/min of He was directed through either a nebulizer (aqueous sample) or headspace generator (organic sample vapor). Also, 2L/min of plasma gas was introduced as the auxiliary flow in order to maintain a stable centered plasma. The flow of N_2 utilized in these studies was 10 mL/min, which contributed to 0.2% of the total volume of gas entering the discharge. All CO_2-doped He plasmas were supplied with a pressure of 100 atm CO_2 which resulted in a decompressed flow rate of approximately 30 mL/min. All plasmas were ignited at and maintained with 150W of forward power and were tuned [13] to minimize reflected power to <3W.

Microwave Cavity

The microwave cavity employed in these investigations was the modified Beenakker TM_{010} resonant type cavity, which is shown in Figure 5. This design is a variant of the original Beenakker cavity in that a translational antenna probe has been installed for ease of critical tuning and more efficient power transfer from the generator to the plasma [3]. This cylindrical cavity was machined from a one inch thick plate of oxygen free high conductivity copper (OFHC). The inner diameter of the cavity is 96 mm, while

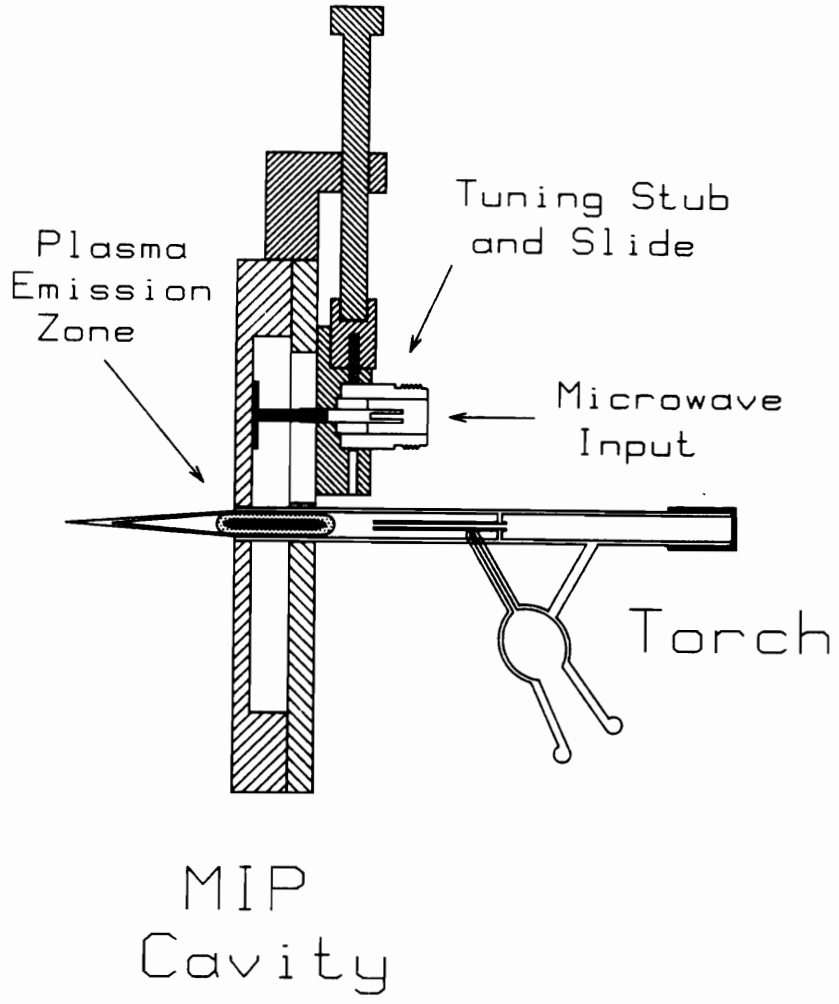

Figure 5: Cross-Sectional View of the Modified Beenakker MIP Cavity

(Adapted from reference 68)

the depth is fixed at 10 mm. This particular version of the modified Beenakker has two 6 mm holes drilled into the end of the structure to allow insertion of two separate quartz tuning rods. However, only one rod was used in these studies. This quartz rod was held in place with a Teflon® set screw which could be loosened to allow changes in penetration depth of the rod relative to the center of the cavity. Movement of the dielectric rod affords critical coupling between the resonant frequency of the cavity and the microwave generator, which has an output frequency of 2450 MHz. An additional 8 mm hole is required in the center of the cavity face plate to allow insertion of the discharge tube.

The back plate of the cavity was machined as a separate piece of 0.2 inch OFHC, as access to the internal portion of the cavity is necessary for repair and cleaning. The plate was attached to the main cavity body with 7 brass flat-head machine screws. An 8 mm hole was drilled through the center of the back plate to allow insertion of the plasma torch. The back plate also had a 0.2 inch X 1.5 inch slot milled out to allow insertion and lateral movement of the antenna coupling disk. Two 1 X 11/2 inch plates were also installed on the back plate to guide the antenna probe, ultimately preventing it from making contact with the back plate on either side of the translational slot. Translation of this probe/disk is essential in achievement of a matched system where the 50 Ω impedance of the generator/transmission cable is matched, by movement of the probe, to a 50 Ω impedance perceived by the capacitively coupled antenna probe inside the cavity. When the system is properly tuned and matched it is said to be "critically coupled".

The antenna probe was constructed from two separate electrical pieces. The 16 mm diameter copper probe disk, which is seated through the back plate to less than 1/8 in from the inside of the cavity face, was silver soldered to a 10 gauge solid copper wire. The probe is coupled to the microwave UG 58 transmission cable by soldering the other end of the copper wire to a UG 58 A/U type N coaxial connector as described by Boss [13]. Two

sides of the coaxial connector were machined to allow the connector to properly fit between the back plate guides. This provided for bind-free translation of the probe.

Microwave Torch

An all-quartz tangential flow plasma torch was generated in our laboratory and utilized in these studies. This torch is represented schematically in Figure 6. The concentric tube design provides for a stable, centered plasma, as the small inner tube helps promote the "corkscrew-type" flow of gas characteristic of tangential flow torches. Probably the most critical feature of this hand blown torch is the angle at which the side arm connects to the main torch body. Since the plasma gas is introduced to the torch through this arm a tangential flow will not be achieved at the required range of flow rates if the angle deviates moderately from 60°.

Optical System

Because He MIP discharges are optically transparent in the radial (side on) mode all of the atomic emission signals were observed in the axial (end on) mode, as shown in Figure 7. The emission was focused onto the entrance slit of either a 0.25 or 0.35 meter monochromator with a f/3 Suprasil® 1-inch quartz lens, and imaged at a magnification ratio of 1:1. A quartz plate was placed over the lens on the side facing the plasma. This prevented the lens from being damaged by the high temperatures which it is inevitably exposed to when collecting light in the axial mode. The photons of interest in the UV-Vis region were collected, and converted to electrical current with the use of a R955 Hamamatsu photomultiplier tube (PMT). Emissions observed in the IR required the use of a red-sensitive PMT, which was also purchased from Hamamatsu. The smaller 0.25 m monochromator was also equipped with a grating blazed at 900 nm. This afforded efficient diffraction and transfer of light in the IR spectral region to the PMT.

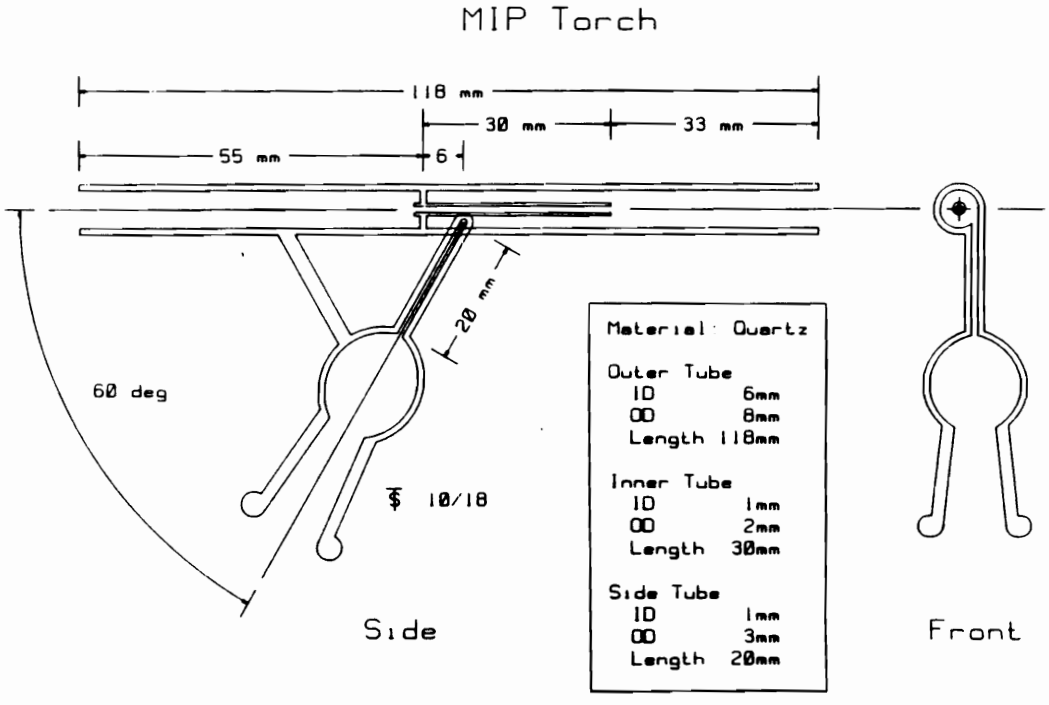

Figure 6: Quartz MIP Discharge Tube (Torch)

(Adapted from reference 37)

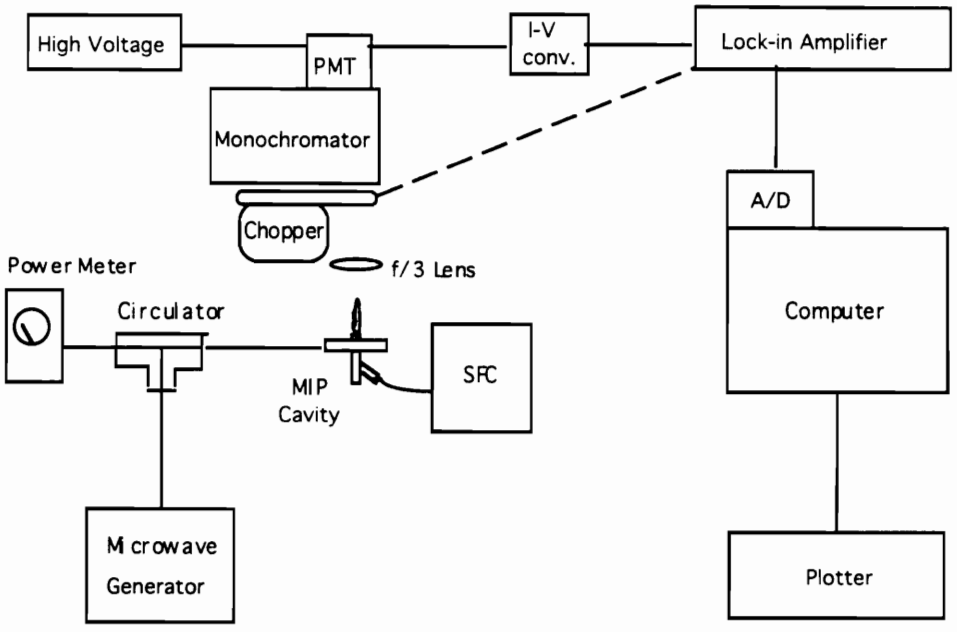

Figure 7: SFC-MIP Instrumental Set-up

Data Collection

The current signals generated by the PMTs were converted to voltages with the use of a EG&G current-to-voltage converter. This analog signal was then transformed to digital form (via A/D converter) so that the spectra could be collected and processed with Chromat-1 data acquisition software run on an IBM 386 computer. By simply moving the vertical cursor to locate the peak maxima, this software allowed accurate measurement of the peak heights directly from the image on the screen.

Table 1: Instrumentation

Component	Model/Size	Manufacturer
Microwave Cavity	HEMIP	Laboratory built
Microwave Generator	HI-2450	Holaday Industries, Edina, MN
Circulator	420IS	Bird Electronic Co.
Power Meter	43	Micro-Now Inst. Co, Chicago, IL
Monochromators	EU-700, 0.35 m 01-512, 0.25 m	Heath Co., Benton Harbor, MI PTI, Princeton, NJ
PMT	R955 R2658 (red sensitive)	Hamamatsu, Bridgewater, NJ Hamamatsu, Bridgewater, NJ
High Voltage Supply	204	Pacific Inst., Concord, CA
12 V Power Supply	EU 601-11	Heath Co., Benton Harbor, MI
Lock-In Amplifier	501	EG&G PARC, Princeton, NJ,
Chopper	125A	EG&G PARC, Princeton, NJ,
I/V	5002	EG&G PARC, Princeton, NJ,
Lens	f/3, Suprasil	Oriel Corp., Stratford, CT
Interference Filter	59523	Oriel Corp., Stratford, CT
Nebulizer	Concentric, TR-50-C2	J. C. Meinhard, Santa Ana, CA
Spray Chamber	Scott type	Laboratory built
SFC System	SFC/200A	Suprex Corp., Pittsburgh, PA
Restrictor	25 μm i.d. Linear	SGE, Austin, TX
Computer	XT 286	IBM, Armonk, NY
ADC Board	Chrom-1-AT	Metrabyte Co., Taunton, MA
Data Acquisition Software	Lab Calc LCCP	Galactic Ind., Salem, NH

Chapter 3

DIAGNOSTIC MEASUREMENTS OF THE HE MIP

With analyses involving atomic emission spectroscopy using plasmas or flames, many processes can occur in the high temperature environment that can affect the efficiency at which the excited state species are populated. It has therefore been necessary to develop and utilize diagnostic methods which are capable of describing the condition of the plasma with respect to temperature and relative populations of plasma species. Such studies are important for the identification of the species thought to play a role in analyte excitation. The diagnostic methods described in this chapter have been used since the late 1960's to evaluate the excitation conditions in a variety of plasma types, including the He MIP. In the current studies plasma diagnostics are applied to monitor temperature changes in a He MIP brought about by the introduction of CO_2

In order to evaluate the physical characteristics of a plasma certain fundamental relationships between plasma species must be obeyed. Basic thermodynamic theory states that a temperature may be defined in a system only if it exists in a state of thermodynamic equilibrium TE. In order for this state to be achieved the following relationships must be obeyed [39,40]:

1) Isothermal equilibrium (IE); where every plasma species must possess the same kinetic energy.

2) Maxwellian equilibrium (ME); where all of the particles have velocities which follow a Maxwell distribution.

3) Boltzmann equilibrium (BE); where the distribution of the population densities of excited states within the same system must obey Boltzmann relationships.

4) Saha equilibrium (SE); which states that the relative population densities of atomic and ionic excited states within the same system (element) follow a Saha distribution.

5) Planks equilibrium (PE); where the distribution of electromagnetic radiation within the plasma must be in agreement with Planck's law

Thus, if all species in a plasma follow these 5 relationships then, theoretically, the plasma can be described by a single temperature.

It is accepted throughout the spectroscopic community that analytical plasmas do not exist in a state of TE. In fact, if Planck's equilibria were to be obeyed any emission of radiation occurring from the de-excitation of an electron would instantly be reabsorbed by the system, eliminating the possibility of any atomic spectrometric measurement. However, a concept that has generated a moderate degree of controversy among spectroscopists is the existence of local thermodynamic equilibrium (LTE). A system in LTE can be defined as that which obeys IE, ME, BE, and SE locally. This means that TE (-PE) is established at each point in the plasma, but the possibility of different temperatures at different points exists. The existence of LTE may also be described as the condition where the rate at which the energy is equally partitioned over the different degrees of freedom is significantly faster than the rate of transport of heat and mass through the plasma [41]. Cogniscant of this situation, researchers have utilized LTE and deviations from LTE to describe physical parameters between analytical plasmas.

Employment of diagnostic measurements based upon LTE has been necessary in these investigations in the attempt to monitor the changes that occur in a He MIP with the introduction of the SFC eluent. Each of the diagnostic methods performed in this study are discussed in detail in subsequent paragraphs. Selection of these techniques was based upon ease and accuracy of the measurement as reported by other researchers. The selected diagnostic methods include determination of excitation temperatures, ionization temperatures, electron number densities, and rotational temperatures.

Excitation Temperature

The excitation temperature is a measure of the relative population distributions of atomic energy levels of a given element. Proportioning between the energy levels is based upon Boltzmann equilibria. The excitation temperature of the He MIP was determined from the spectral emission intensities of a variety of spectrometric species. Details of the selected elements and emission lines are presented in chapter 5. The Boltzmann relationship used to calculate T_{exc} from each of the spectrometric probes is presented below:

$$T = \frac{(E_1 - E_2) \,/\, 2.30\, k}{\log (A_1\, g_1\, \lambda_2 \,/\, A_2\, g_2\, \lambda_1) \;-\; \log (I_2 / I_1)}$$

Where:

E = excitation energy
A = transition probability
g = statistical weight
λ = wavelength
k = Boltzmann constant $(6.24 \times 10^{18}$ eV/K)

Here, the subscripts 1 and 2 represent the two emission lines. While this expression demonstrates the calculation of temperature with just 2 emission lines, it can be rearranged to calculate the excitation temperature using more than two lines. The spectrometric constants used in calculating T_{exc} with each of the different probe species are listed in Tables 2-4.

Electron Number Density

Determination of the electron number density of the He MIP was performed by employing the method of Stark broadening [42]. This method relies upon several conditions induced in the plasma as a result of the presence of electrons. Electrons in a plasma create an electric field which polarizes the hydrogen atom. This interaction removes energy level degeneracy and causes a splitting of levels (via the Stark effect) to occur. This splitting of energy levels results in each of the states emitting radiation at slightly different wavelengths. Thus, the Hβ line appears to broaden proportionally to the number of electrons present in the discharge. The broadening of the peak is measured as the full width at half height (FWHH). While atoms other than hydrogen experience Stark broadening under similar conditions, atomic hydrogen lines are the most frequently used for this measurement, as the availability of the Stark broadening parameters is relatively high.[38].

Selection of the Hβ line, using FWHH, provides several advantages over other hydrogen lines, thereby permitting n_e^- to be calculated as follows:

$$n_{e^-} = c\,(n_{e^-}, T)\,(\lambda_S)^{3/2}$$

Here, c (n_{e^-}, T) is a function of the density of electrons (per cubic centimeter) and temperature, and λ_S is the FWHH of the Hβ line. Values of c (n_{e^-}, T) can be found in tabulated form in a book composed by Griem [42].

Ionization Temperature

The ionization temperature represents the equilibrium between atomic and ionic excited states of the same element. This distribution is governed by the Saha-Eggert relationship [29,43]:

$$[(I_i/I_a) = [4.83 \times 10^{15}/n_e] (g_pA_{pq}/\gamma)_i(\gamma/g_pA_{pq})_a \times T^{3/2} \times \exp[(-E_i - E_{pi} + E_{pa}) / kT]$$

Where: I_i = ion line intensity
I_a = atom line intensity
n_e^- = electron number density (electrons per cubic centimeter)
g_p = statistical weight of level P (upper level)
A_{pq} = transition probability of the p-q transition (s^{-1})
γ = Wavelength of pq transition (nm)
E_i = ionization energy (eV)
E_{pi} = excitation energy of level p (ion) (eV)
E_{pa} = excitation energy of level p (atom) (eV)
k = Boltzmann constant
T = ionization temperature (K)

The measured relative intensities of the ion and atom lines, n_e-, and T_{exc} are entered into a Basic computer program and, through an iterative process, the ionization temperature is calculated. Table 5 shows some common wavelengths and constant values used in this determination.

Table 2:

Spectrometric Constants of He used in Excitation Temperature Determinations

Wavelength (nm)	E_p	gp	A_{pq} (10^8)
388.87	185565	9	0.09478
447.15	191445	15	0.246
471.31	190298	3	0.0955
501.57	186210	3	0.1338

Table 3:

Spectrometric Constants of Fe used for Determination of Excitation Temperature

Wavelength (nm)	Ep (cm^{-1})	gp	Apq
370.5	27395	7	0.033
372.2	27560	5	0.050
373.5	33695	11	0.886
374.8	27560	5	0.090
375.8	34329	7	0.611
382.0	33096	7	0.638
385.6	45295	11	0.87
389.6	49461	11	0.14
390.0	51771	7	0.086

Table 4:

Spectrometric Parameters of Cl used in Excitation Temperature Determinations

Wavelength (nm)	gm	A_{mq} (10^8/s)	E (ev)
384.542	5	0.94	19.173
384.569	3	2.0	19.173
384.584	1	2.7	19.173
385.102	7	1.8	19.173
385.142	5	1.6	19.173
385.169	3	0.67	19.173
386.083	9	2.7	19.173
386.099	7	0.89	19.173
386.134	5	0.18	19.173
423.409	5	0.36	18.877
424.138	5	0.60	18.877
425.351	5	0.84	18.877
434.632	5	0.84	18.575
479.454	7	1.18	15.963
481.006	5	1.13	15.952
481.946	3	1.11	15.949
489.677	9	0.88	18.253
490.476	7	0.81	18.244
491.772	5	0.75	18.234
521.794	5	0.77	16.339
522.134	3	0.77	16.338
542.325	7	0.18	15.963
542.352	7	0.037	15.963
542.436	7	0.0056	15.963
544.342	5	0.15	15.954
544.425	5	0.095	15.954
544.499	5	0.024	15.954
545.627	3	0.084	15.949
545.702	3	0.11	15.949
545.747	3	0.048	15.949

Adapted from reference 55

Table 5:

Spectrometric Constants of Ca and Cd used in Ionization Temperature Determinations

Species	Wavelength (nm)	E_q (cm^{-1})	gp
Ca I	422.7	23652	3
Ca II	396.8	23192	2
Cd I	228.8	43692	3
Cd II	226.5	44136	2

Chapter 4

THE EFFECT OF H_2 AND CO_2 ON NON-METAL EMISSION LINE INTENSITIES IN A HELIUM MICROWAVE - INDUCED PLASMA

The driving force behind the ongoing development of the He MIP as an element selective detector for SFC has been described in Chapter 1. Also mentioned was the negative effect of introducing gases other than the main plasma gas. The current chapter will describe efforts in determining the effect of H_2, which was thought to provide signal enhancement, and CO_2 on a He MIP. This was accomplished by monitoring non-metal emissions and diagnostic temperatures of the plasma with and without the introduction of these gases. The results presented in this chapter reveal the direct relationship between non-metal signal depression, brought about by the introduction of CO_2, and transition energy. In particular, data on Cl, Br, I, S, and P will be presented. Initial attempts at monitoring the change in plasma energy through excitation and ionization temperatures are also described. The unexpected signal depressing effects of H_2 are presented as well.

For comparative purposes, it is important to consider the effect of CO_2 on a low powered Ar MIP. As described in the introduction, the electron number density and excitation temperature of an Ar discharge were shown to significantly decrease with the introduction of supercritical CO_2 at flow rates similar to those incorporated in the work presented in Chapeters 4 and 5. These findings will serve as a reference for evaluating the applicability of diagnostic methods to the He MIP

RESULTS AND DISCUSSION

Effect of CO_2 and H_2 on Non-metal Emission Line Intensities

An extensive investigation on non-metal line selection in a He MIP has been performed by Tanabe *et al.* [44]. The wavelength region from 190-850 nm was monitored for atomic and ionic emission signals that were observed in the plasma. The relative intensities and energies of these transitions, along with interfering molecular emission bands, were reported. It is this compilation of data, in addition to results reported in recent communications of Carnahan Hieftje, and Jones [45,46] dealing with He-non-meal charge transfer in helium plasmas, that served as a guideline for initial non-metal selection in the present study. The electronic transitions observed in our plasma roughly agree with those observed in similar plasmas. However, the relative intensities of these emission signals were not in total agreement. As a result of these minor discrepancies between this plasma and others, the non-metal lines selected for these studies were those transitions that yielded the most intense ionic and atomic emission signals.

In the present work, the effect of the introduction of CO_2 and H_2 to a He MIP on the non-metal atomic and ionic emission intensities of Cl, Br, I, S, and P is examined. This data is presented in Table 6 and is discussed in the following paragraphs. The loss in non-metal emission signal caused by the addition of the gases is expressed as a percentage. This value is based upon the 100% signal obtained from the analytes in the pure He plasma.

Chlorine

The chlorine emission lines monitored for determination of the effect of CO_2 and H_2 were the 725.7 nm atom line and the 479.5 nm ion line. The source of chlorine signal was chloroform vapor, which was produced with the headspace generator. The atomic line is a result of a transition possessing a total energy of 10.63 eV, while the ionic line is from a transition demanding 28.97 eV of total energy [44]. It should be noted that the ion line

generated in this 150W plasma is 5.6 times more intense than the atom line. As listed in Table 6, the ionic signal is found to exhibit a more significant depression than that of the atomic signal with the addition of either of the gases. The introduction of CO_2 to the He MIP results in a 46% loss in ionic signal, while a 64% signal loss is observed with the addition of H_2. The introduction of both gases causes a 74% attenuation of the ionic signal. A similar yet less significant, loss is noted for the atomic chlorine line: an 18% loss with CO_2, a 22% loss with H_2, and a 36% loss with the addition of both gases.

Bromine

The atom and ion lines utilized for the analysis of Br were at 734.8 nm and 478.6 nm, respectively. The atomic line results from a transition requiring a total energy of 9.73 eV. 26.15 eV was required for the Br ionic transition [44]. The constant Br signal was produced from headspace generation of 1-bromopropane vapor. In this 150W plasma, the ion line was found to be 2.3 times the intensity of the atom line. As with the chlorine data, the Br ion line yielded a greater signal depression than the atomic line with the addition of CO_2 and H_2. Also, similar trends in signal depression with the introduction of both gases is noted and shown in Table 6.

Iodine

Diiodomethane vapor, swept into the plasma through the headspace generator, served as the emission signal of iodine. The most intense ionic and atomic transitions observed for this element in the He discharge correspond to 540.6 nm and 206.3 nm, respectively, and the ion/atom ratio for these emission lines was 0.05. The atomic line resulted from a transition requiring a total energy of 6.95 eV, while the ionic line resulted from a transition utilizing 24.36 eV of total energy [44]. As was observed with Cl and Br, the ionic signal is more significantly affected by the introduction of H_2 and CO_2 than the

atomic line. The introduction of CO_2 resulted in a 30% depression for the ion line and a 10% reduction of the atomic line. The introduction of H_2 resulted in a more severe series of depressions: 37% for the ion, and 19% for the atom. The combined effect of both gases yielded a 47% reduction of the ionic signal and a 30% loss in the atomic signal. These results are displayed in Table 6.

Sulfur

The introduction of carbon disulfide vapor into the plasma provided a sufficient source of sulfur emission. The lines selected for these analyses were the atom line at 921.3 nm and the ion line at 543.3 nm. 7.87 eV were needed to promote the atomic sulfur transition, while the ionic line occurred from a transition demanding 26.25 eV of total energy [44]. Measurements conducted with the two spectroscopic systems yielded an ion/atom ratio of 0.7 in the pure He plasma. Contrary to the other elements and transitions studied, the introduction of CO_2 into the He plasma did not result in a signal loss for the atomic line. However, the ionic line did decrease in emission intensity by 21% with the introduction of CO_2. The addition of H_2 and a mixture of H_2 and CO_2 resulted in an attenuation of the atomic and ionic signals as listed in Table 6.

It is important to note that the addition of CO_2 yields a sulfur atom line which is essentially unaffected, as the energy associated with its electronic transition is relatively low. Because the ion/atom ratio approaches 1 for the 543.3 nm and 921.3 nm emission lines it seems logical that selection of either line would provide adequate quantitative measurements. However, a closer look at the interference of the ion line brought about by the introduction of mobile phase reveals that the 921.3 nm atom line is much more suitable for analytical determinations.

Phosphorus

The effect of chromatographic gases on the signal intensities of P was determined by introducing triethyl phosphate vapor into the plasma and monitoring the atom line at 253.6 nm and the ion line at 458.9 nm. The atomic line resulted from an electronic transition requiring 7.21eV, while the ionic line occurred from a transition of 26.78 eV of total energy [44]. Examination of Table 6 reveals that both P transitions experienced essentially the same degree of signal depression with the introduction of each gas: 30% with CO_2, 60% with H_2, and 60% with addition of both gases. It is thought likely that a reaction is taking place in the plasma with P which is affecting the relative populations of the excited P states. In any case, these observations are contradictory to the depression trends observed with the other nonmetals under investigation. It should be noted that Estes *et al.* reported signal enhancement of P, in addition to a series of metals, in a He MIP with the introduction of H_2 [9]. This increase in emission signal was attributed to the prevention of elemental deposition onto the inner walls of the discharge tube. In this way, the addition of H_2 effectively cleanses the walls of the discharge tube, forcing the analyte to remain in the observation region where it can be excited and detected.

Signal Depression and Total Transition Energy

As shown in Table 6, the ionic transitions of the non-metal ion/atom pairs are most affected by the introduction of chromatographic gases into a 150W He MIP. An explanation for this phenomena is that the ionic transitions require a large amount of energy to generate emission signals relative to the atomic transitions. This trend is shown to be the case for the non-metal ion/atom/ line pairs studied in this work as well as the Cl emissions examined by Carnahan [6]. However, in order to effectively evaluate the relationship between signal depression and transition energy one needs to consider a larger series of

Table 6:

Effect of Chromatographic Gases on Non-metal Emission Intensities

Element	Line (nm)	Transition Energy (eV)*	% loss with CO_2	% loss with H_2	% loss with CO_2/H_2
Cl	725.7 (atom)	10.63	18	22	36
	479.5 (ion)	28.97	46	64	78
Br	734.8 (atom)	9.73	33	36	48
	478.6 (ion)	26.15	46	55	60
I	206.2 (atom)	6.95	10	19	30
	540.7 (ion)	24.36	30	37	47
S	921.3 (atom)	7.87	0	9	18
	543.3 (ion)	26.25	21	31	48
P	253.6 (atom)	7.21	32	62	61
	458.9 (ion)	26.78	35	60	55

CO_2 flow rate = 30 mL/min decompressed

H_2 flow rate = 100 mL/min

CO_2/H_2 = 0.3

* from Tanabe *et al.*, ref 44.

Electronic transitions listed are those which give rise to the observed emission. The energies listed are total energies for the transitions as measured against ground atomic state.

transitions within a single element, since comparisons between different elements reveals no absolute correlation.

Six Cl transition were monitored with the introduction of CO_2 in an attempt to describe the relationship between signal depression and total transition energy. Three of these selected transitions are due to atomic states and three represent ionic transitions. The signal intensities of each of these lines in a 150W pure He plasma were recorded and compared to signal intensities produced by the CO_2-doped He plasma. The signal reduction observed with the six chlorine lines is shown in Figure 8. Here, % signal depression is plotted against total transition energy for each of the lines studied. The three data points on the lower left hand side of the figure represent atomic lines, while the points in the upper right hand portion are due to ionic transitions. As shown on the figure, a steady increase in signal depression is noted with an increase in total transition energy. The gap in the plot from roughly 15-27 eV is not intentional, but results from the lack of available Cl transitions existing within this energy range. For comparative purposes it is important to note that the energy required to promote ionic transitions from the ground ionic state to a particular excited ionic state is added to the ionization potential(energy) of that element. The result is a representation of the total transition energy.

Effect of CO_2 on Excitation Temperatures.

The introduction of carbon species into analytical plasmas has been shown to decrease the analyte exciting ability of both He and, to a much larger extent, Ar plasmas [2]. It has been suggested that a significant portion of the plasmas energy is consumed in dissociation of the carbon containing molecules which results in a decrease in the atomic emission signals of the analyte results [29]. However, the exact mechanism by which carbon species affect the populations of excited state species has not yet been unambiguously determined.

Figure 9 demonstrates the effect of the addition of 100 atm (25 mL/min) of CO_2 on a He MIP. Here, the excitation temperature is monitored as a function of applied power and gas composition. The T_{exc} is found to not deviate significantly from a value of 4950K with increasing forward power in a pure He plasma. The temperature of the CO_2-doped He plasma was determined to be slightly lower (4800K) than the pure He plasma. The largest difference in T_{exc} between the two plasma types occurred at 300W of applied power. This approximately 4% discrepancy should not be considered significant as the error associated with these calculations has been accepted as 3%. It should be noted that the reduction in T_{exc} with the introduction of CO_2 is not due to a loss of critical coupling between the plasma and the generator, as this would have resulted in a significant increase in reflected power and heating of the cavity. Since neither of these effects were observed, the slight reduction in T_{exc} cannot be attributed to a change in the efficiency of power coupling.

Effect of CO_2 on Ionization Temperature

The effect of the addition of 100 atm of CO_2 on the ionization temperature of a pure He plasma is shown in Figure 10. The T_{ion} values were determined from the Saha-Eggert relation which, in this particular system, utilized the atom and ion emission lines of Cd, and the electron number density was determined by the Stark method. The n_e^- maintained a relatively constant value of 1.0×10^{15} electrons per cubic centimeter for the He and He/CO_2 plasmas at all forward powers studied. As demonstrated in Figure 10, a slight increase in T_{ion} of both plasmas with higher applied power is evident. Additionally, a slight increase in T_{ion} of the He/CO_2 plasma, relative to the pure He plasma, is observed at lower applied powers. This difference in T_{ion} between the two plasmas tapers off at

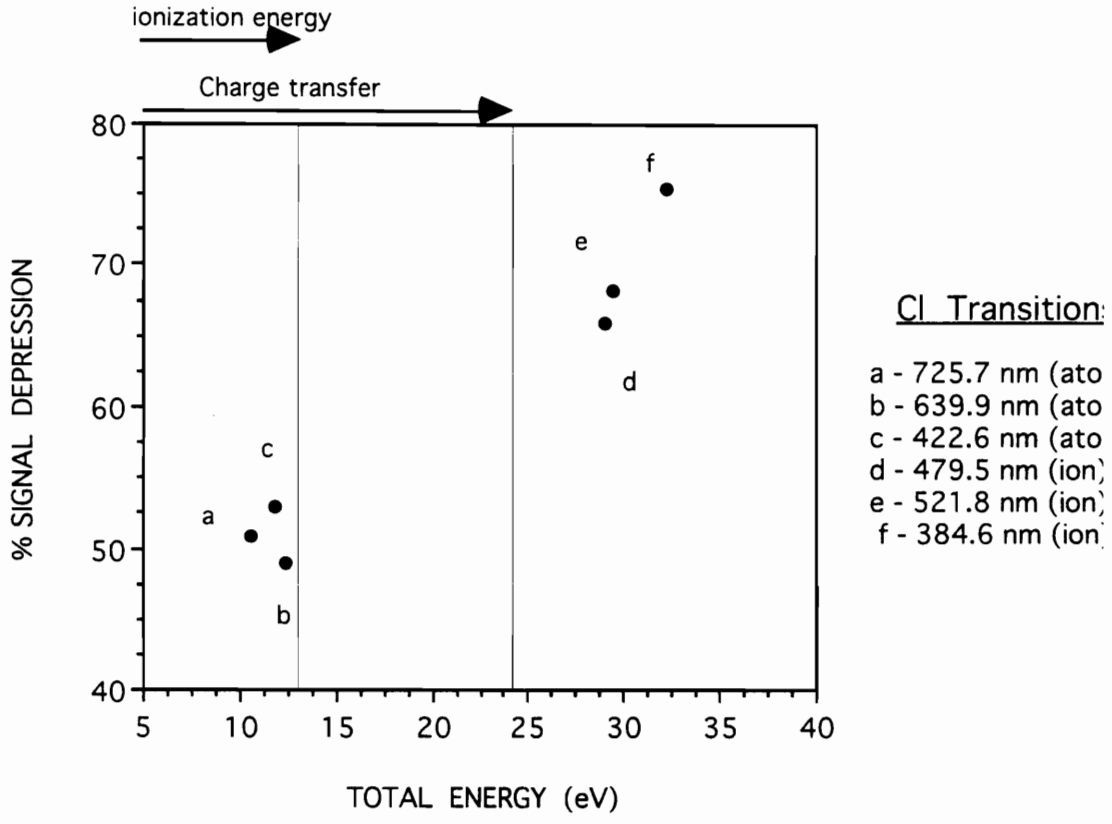

* ionic species result from ionization energy + transition energy

Figure 8: Plot of Signal Depression vs. Total Transition Energy for 6 Cl Lines.

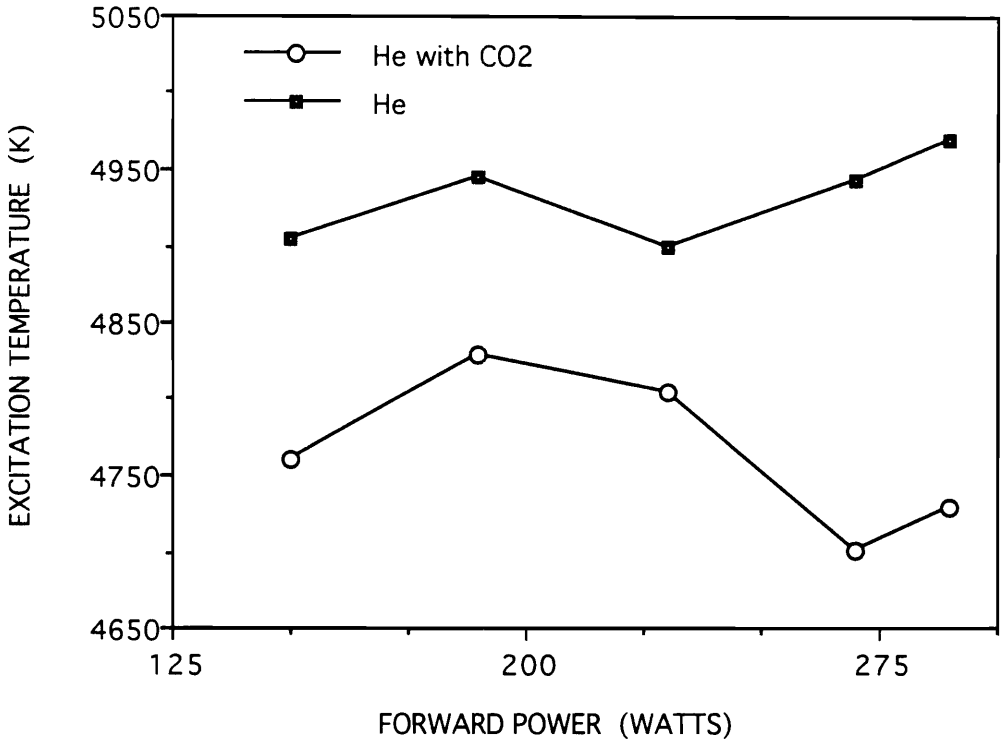

Error associated with these calculations is ~3%

Figure 9: Effect of CO_2 on Excitation Temperature of the He MIP.

higher forward powers. It should be noted that the changes in T_{ion} between the He and CO_2-doped plasmas represents no more than a 2% deviation in calculated value for T_{ion}. Given the uncertainty in these measurements, these differences are determined to not be statistically different.

As with the T_{exc} determinations, the reduction in T_{ion}, as a consequence of the introduction of CO_2, is not likely to be due to a loss in critical coupling of the system. Rather, the presence of this mobile phase in the plasma results in a loss of energy in the discharge.

Effect of H_2 on Excitation Temperature

It has been demonstrated in several works that the addition of hydrogen to a He MIP proves a viable method for signal enhancement and extension of the linear dynamic range (LDR) of the technique for certain elements [9,10]. These improvements are thought to be achieved through the physical and/or chemical events taking place in the plasma that serve to rid the discharge tube walls of analyte-containing deposits which effectively decrease the amount of elemental species excited in the discharge. Signal enhancement in SFC-MIP analyses, where the introduction of mobile phase results in absorption of plasma energy and a subsequent depression of analyte signal, could prove beneficial at recovering some of the emission signal. Selection of the H_2 flow rates was based upon the relative proportion of organic vapor entering the plasma as well as flow rates utilized in a similar study by Hubert with a surfatron MIP.[10]. The flow rates employed in the current studies are 100 and 500 mL/min. The former flow rate contributes to 1.5% of the total gas flow entering the discharge tube, while the latter represents 7.5% of the total flow. As can be seen from Figure 11, the introduction of both H_2 flows results in a slight decrease in T_{exc} at 150W and an unchanged or greater value of T_{exc} for each of the higher forward powers

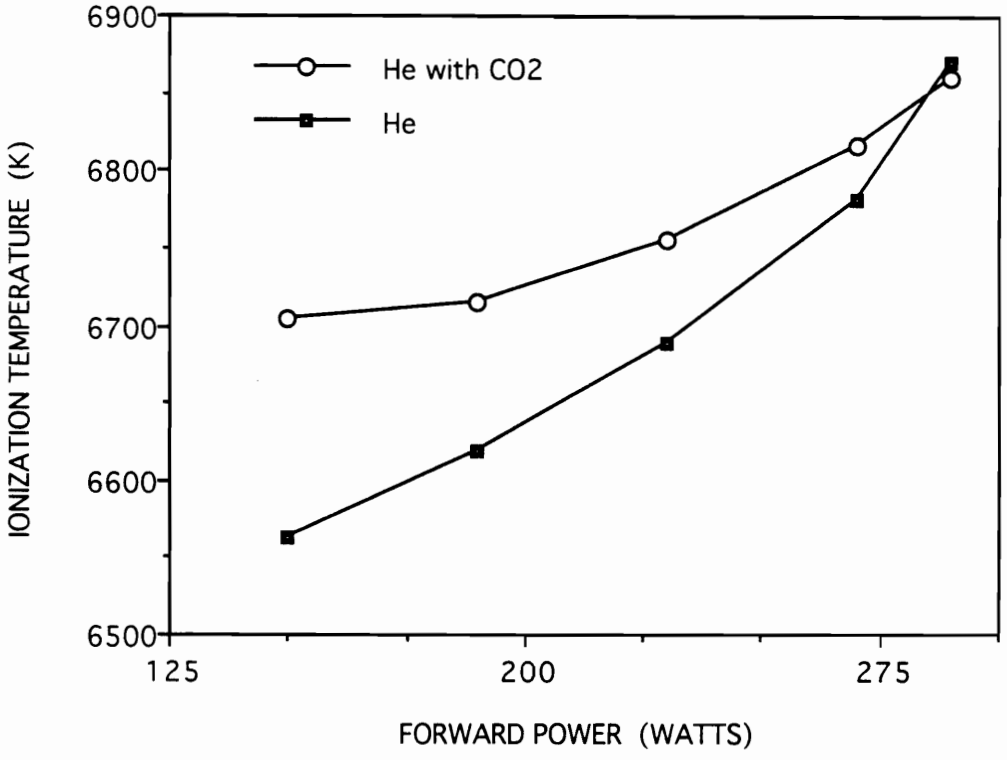

Error associated with these calculations is ~3%

Figure 10: Effect of CO_2 on Ionization Temperature of the He MIP.

relative to the pure He plasma. Only the addition of 7.5% H_2 at the lower powers caused an increase in T_{exc} greater than the error associated with the method of measurement.

Effect of H_2 on Ionization Temperature

Figure 12 demonstrates the effect of the addition of 1.5 and 7.5% H_2 on a helium plasma. As was performed with the previous T_{ion} calculations, the n_{e^-} values of the plasma were first measured with the addition of H_2. The lower flow of H_2 resulted in an electron number density of 1.1 $X10^{15}$ e^-/cc over the entire power range studied. Addition of the 7.5% H_2 flow yielded a ne^- of 1.4 $X10^{15}$ e^-/cc for the 150 W plasma, while a value of 1.3 $X10^{15}$ e^-/cc was obtained at the 300 W level. As with the T_{exc}, the T_{ion} of the He MIP falls with added H_2 at 150W but increases to values approaching the pure He plasma at higher forward powers. Similar to the effect of CO_2, the addition of H_2 causes a slight enhancement in T_{ion} at most forward powers.

Effect of Added Gases on Plasma Geometry

It could be argued that the observed reduction in emission intensity of the nonmetal transitions studied in the He discharge is not a result of the decreased population of excited state species but may be a perturbation of the plasma geometry. It is possible that the introduction of CO_2 and/or H_2 is affecting the normal analytical viewing zone of the He discharge. If this situation were to occur, the so called signal depression could be explained by the inadvertent observation of a different region of the plasma, one which does not generate emission signals as intense as the original viewing zone in the pure He plasma. This effect was investigated by performing axial emission scans of the chlorine ionic transition (479.5 nm) in a 150W plasma with and without the introduction of the chromatographic gases. These scans are depicted on Figure 13. The 0 mm position

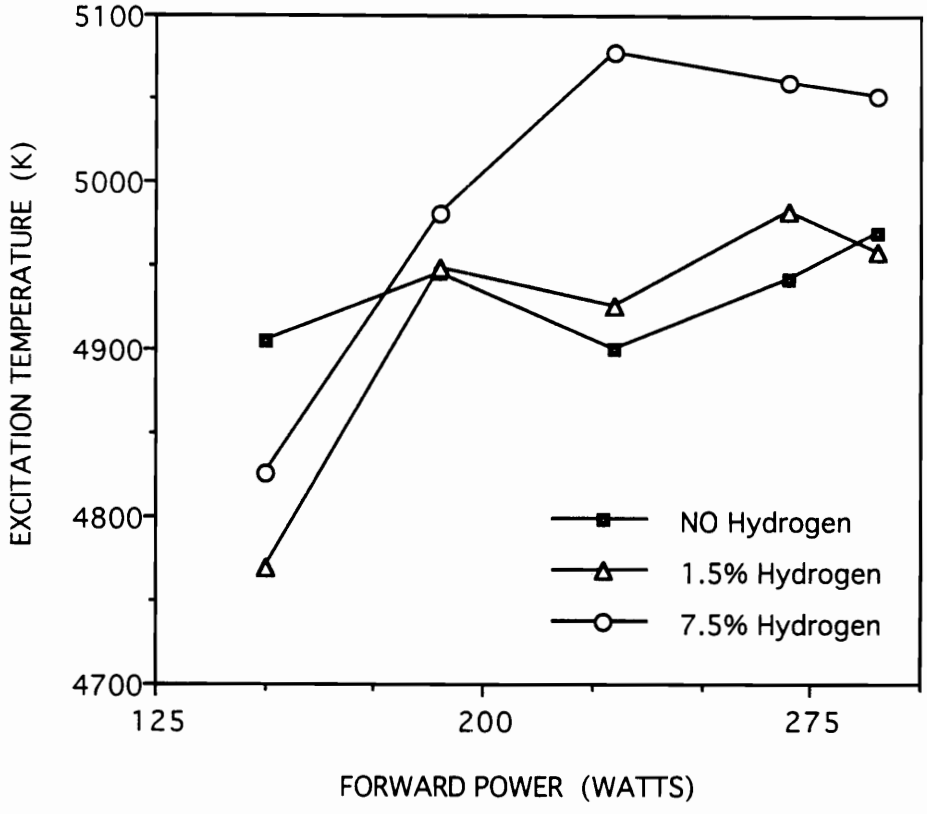

Error associated with these calculations is ~3%

Figure 11: Effect of H_2 on Excitation Temperature of the He MIP.

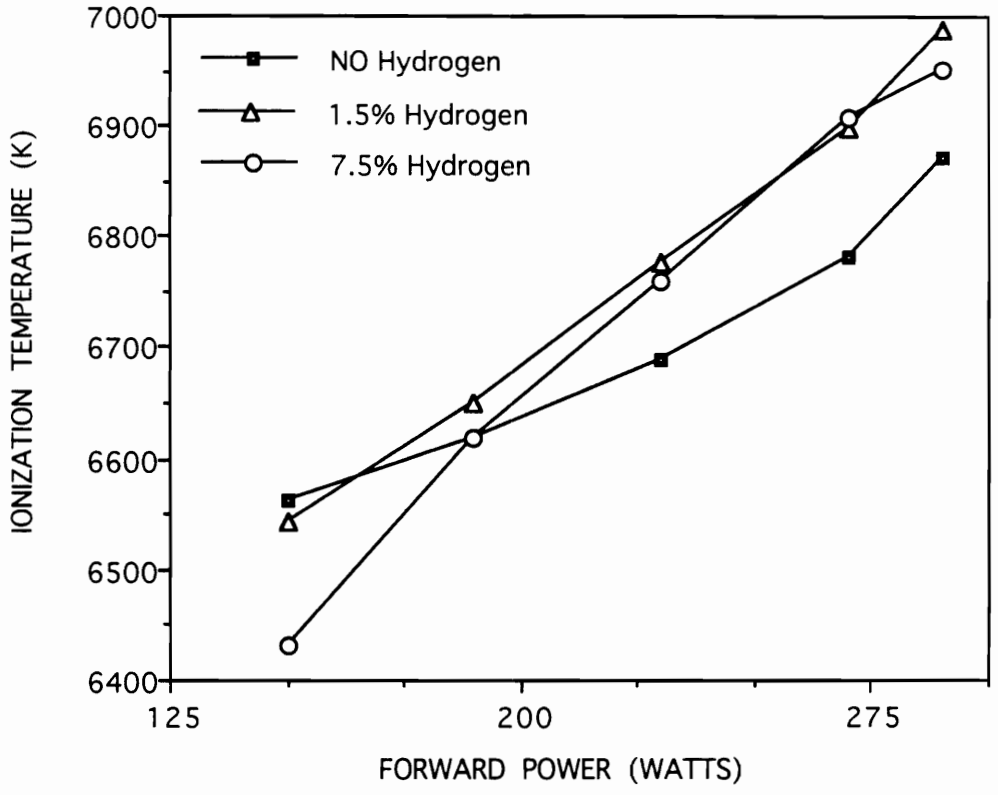

Error associated with these calculations is ~3%

Figure 12: Effect of H_2 on Ionization Temperature of the He MIP

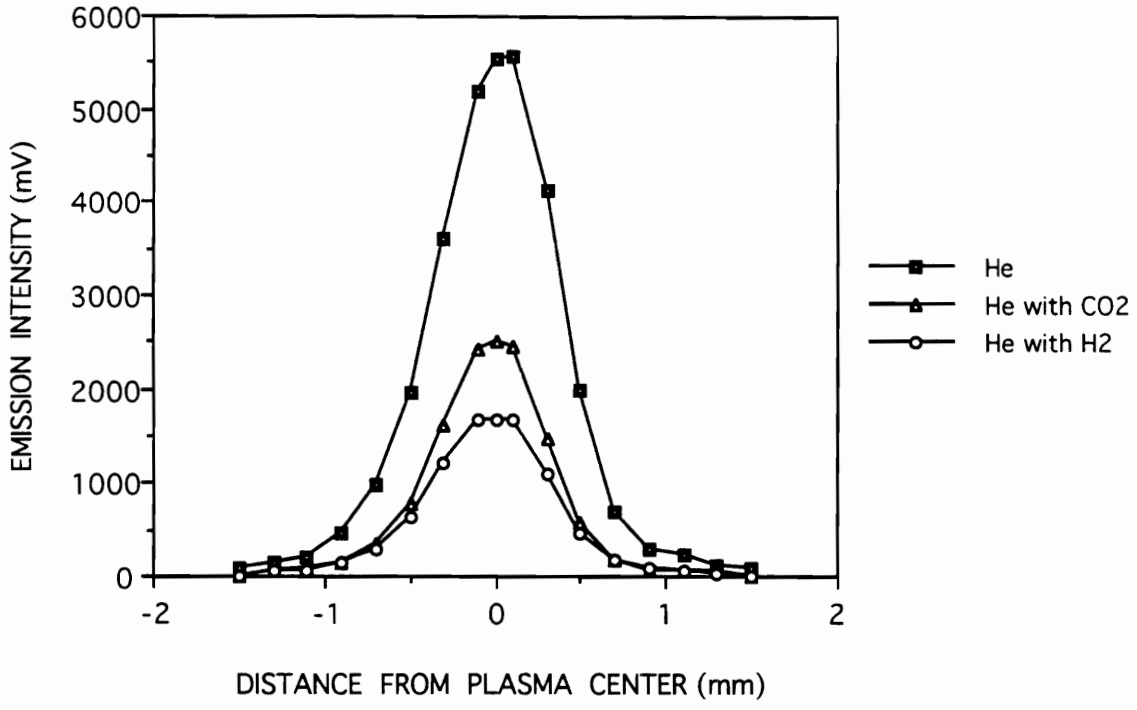

Figure 13: Axial Scan of Cl Emission at 479.5 nm

corresponds to the center of the He discharge generated in the 5 mm i.d. torch. Although the addition of CO_2 results in a 46% depression of the chlorine signal, no shift in emission maxima is evident. The addition of 7.5% H_2 yields a 70% signal depression with no change in the viewing zone for the position of maximum chlorine emission. These results indicate that no physical shift of the optimal viewing zone occurs with the addition of either of the chromatographic gases. Therefore, the loss of emission signal is not due to a geometric perturbation of the plasma but is, in fact, the result of a decreased efficiency of the plasma in promoting the population of excited states.

SUMMARY

The addition of CO_2 and H_2 to a He microwave-induced plasma is found to diminish the excitation properties of the 150W discharge. While the excitation and ionization temperatures do not indicate a significant alteration of the plasmas energy with addition of the gases, substantial depressions of certain S, Cl, Br, and I emission signals suggest that a significant loss or redistribution of energy is taking place. Additionally, the higher degree of signal depression experienced by the ion line relative to the atom line for each of the non-metals studied suggests a direct relationship between transition energy and stability of a particular electronic transition. Analysis of six chlorine emission lines clearly demonstrates the relative instability of higher energy transitions and the direct correlation of transition energy and signal depression. A more detailed look at the processes which are affected by the presence of foreign gases in a He MIP is presented in Chapter 5. These investigations have demonstrated that while certain non-metal electronic transitions are significantly affected by the introduction of CO_2 and/or H_2, careful selection of emission lines can provide for reliable, quantitative spectrometric detection of non-metals in SFC-MIP. Electronic transitions that yield strong emission in pure He plasmas may not

serve as accurate indicators of the analyte population in gas-doped He discharges if the line results from a high energy transition. This change in signal intensity could be most problematic during a chromatographic run that employs pressure programming of the supercritical fluid mobile phase. Applying this mode of SFC introduces varying concentrations of mobile phase which could add substantial systematic error to analyses as unstable high energy transitions "feel" this change in CO_2 flow. Hence, the total transition energy as well as the emission line strength should both play a role in line selection when employing element specific detection SFC-MIP.

Meanwhile, the addition of H_2 to a He MIP yields no signal enhancement for the elements and transitions studied. In fact, these observations contradict those obtained with GC-MIP systems. This discrepancy may be due to the different torch designs employed in the compared studies. The current study utilizes a relatively large i.d. discharge tube (5 mm) while the investigations performed by Uden *et al.* employ 1 mm i.d. plasma tubes. The presence of surface interactions between the analyte and the inner walls of the torch with the latter design may not be occurring with the larger i.d. tube used in these studies. In this case the introduction of H_2 into a 150W He MIP would not serve to counter the decreased analyte emission brought about by the SFC mobile phase.

Chapter 5

A COMPARATIVE STUDY OF DIAGNOSTIC METHODS FOR DETERMINING THE EFFECT OF CO_2 ON A HELIUM MICROWAVE-INDUCED PLASMA

The previous chapter described the effect of the introduction of supercritical CO_2 to a He MIP on the non-metal emissions. Chapter 4 also described attempts to monitor the change in energy of the He MIP with the introduction of this SFC mobile phase. The measured plasma ionization and excitation temperatures indicate that no decrease in plasma energy is occurring with the introduction of supercritical CO_2. However, the observations of reduced non-metals emission intensities in the presence of CO_2 demonstrate that a reduction in the available excitation energy of the plasma is occurring. Therefore, in the current chapter a variety of spectrometric species for determination of T_{exc} and T_{ion} will be persued. Additionally, the measurement of plasma rotational temperatures utilizing the OH radical and N_2^+ rotational bands with and without the introduction of CO_2 will be discussed. Realizing the limitations of LTE-based measurements, this chapter will apply a recently developed theory on charge transfer to model the energy reduction of a He MIP, as conventional diagnostics fail at this task. Finally, the influence of kinetic data involving reactions of He plasma species will be considered, as this may provide a further understanding of the excitaiton processes that take place in a He MIP.

RESULTS AND DISCUSSION

Excitation Temperature

A commonly employed diagnostic measurement for evaluation of analytical plasmas is the excitation temperature (T_{exc}). As described in Chapter 2, determination of T_{exc} involves monitoring a series of atomic transitions of a particular element which is introduced

into the plasma as a probe. The relative intensities of these excited electronic states can be related to population distributions through the use of the Boltzmann equation. In many instances the availability of spectrometric constants determines which probe species will be employed. Most commonly He and Fe are employed as the spectrometric species. This study will determine the excitation temperatures with the use of He, Fe, and Cl.

Fe

The first spectrometric probe investigated in these studies was the metal iron. The Boltzmann plot generated with the intensity measurements of the Fe 371.99 nm, 373.49 nm, and the 373.71 nm lines is not represented, yet the resulting T_{exc} is displayed in Table 7. Comparison of T_{exc} determined with Fe between the pure He plasma and the He/CO_2 plasma indicates a 3% decrease in temperature with the addition of 100 atm of mobile phase. A log-log plot of Fe intensities in the pure He plasma vs Fe intensities in the He/CO_2 plasma yields a straight line with a slope near that of 1. This method, which is designed to determine if two sets of data are statistically different, indicates that the T_{exc} values measured in the two different plasmas are statistically the same.

He

The next spectrometric species evaluated was that of a noble gas. Boltzmann plots of the He emission intensities measured in the He and He/CO_2 plasmas indicate a 6% increase in the T_{exc} with the CO_2-doped He plasma (Figures 14,15). Based upon the 3% error inherent in these temperature calculations, the differences in T_{exc} for the He and He/CO_2 plasmas does not appear to be significant with the He probe. Additionally, a statistical plot was generated with these data (Figure 16). As with the Fe species, log - log

Table 7:

Summary of Diagnostic Values

Measurement	Spectrometric Species	Pure He Plasma	He/CO_2 Plasma
Excitation Temperature	Fe	4,900 K	4,760 K
	He	4,860 K	5,170 K
	Cl	10,400 K	11,600 K
Ionization Temperature	Cd	6,500 K	6,700 K
	Ca	6,700 K	6,870 K
Rotational Temperature	OH	2,220 K	‡
	N_2^+	3,490 K	‡
Electron Number Density (e^-/cc)	$H\beta$	$1.2*10^{15}$	$1.2*10^{15}$

Error in the temperature measurements is approximately 3%.

‡ interference prevented measurement with the introduction of CO_2

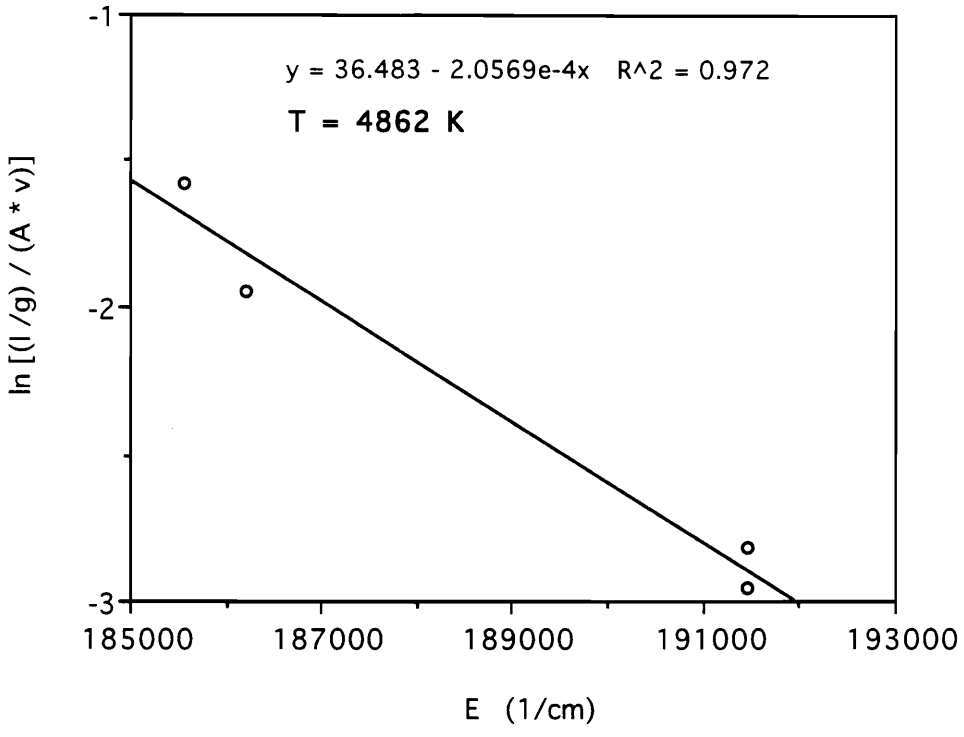

Figure 14: Boltzmann Plot of He Line Intensities for the Pure He MIP.

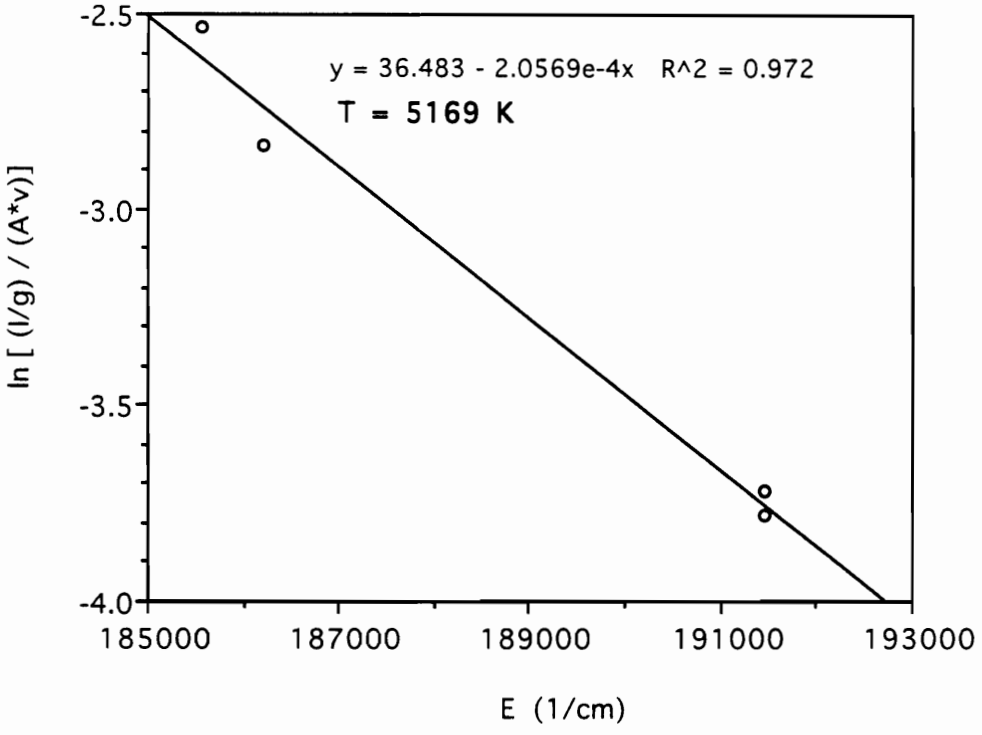

Figure 15: Boltzmann Plot of He Line Intensities for the He/CO_2 MIP.

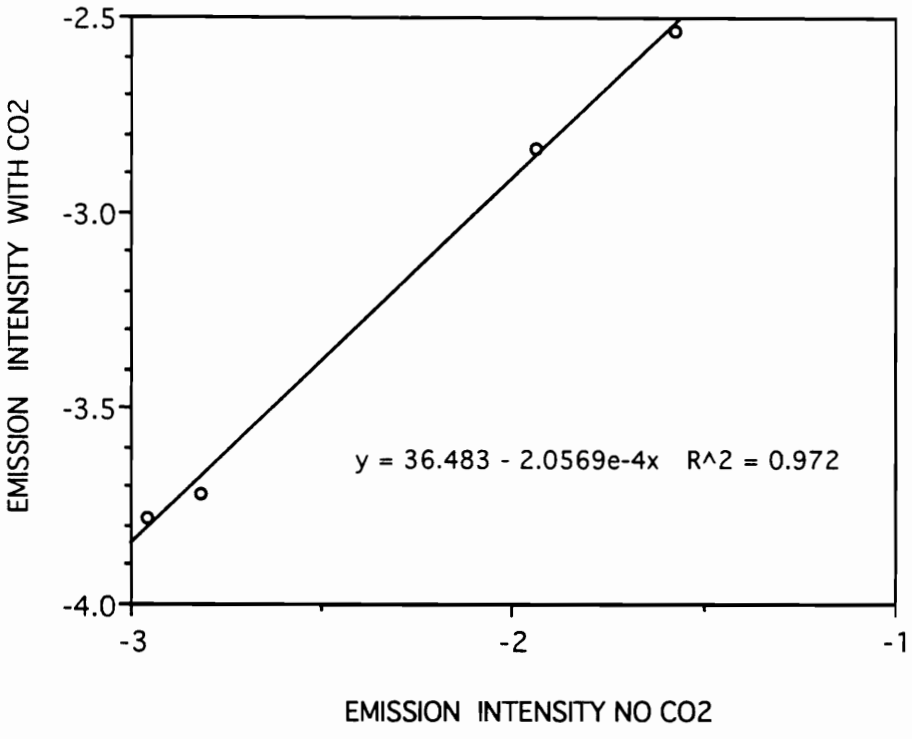

Figure 16: Slope Comparison of He Line Intensities for He and He/CO_2 MIP.

plots of He data yield a line with a slope approaching a value of 1 [47]. Again, this is evidence that the T_{exc} obtained with each plasma are not statistically different.

Cl

Excitation temperature determinations performed with the metal and noble gas probes do not seem to accurately represent the energy state of the He MIP in the presence of SFC mobile phase. Because the introduction of CO_2 has been shown to significantly effect the emission intensities of non-metal transitions, it was thought likely that T_{exc} incorporating a non-metal spectrometric species would serve as a more accurate determination relative to He or Fe. The Cl lines selected for these analyses were the 489.68 nm, 490.48 nm, 491.77 nm, 521.79 nm, and the 552.13 nm transitions. Comparison of the pure He and the He/CO_2 Boltzmann plots reveals a 10% increase in Cl excitation temperature with the addition of CO_2 (Figures 17, 18). The statistical log-log plot results in a slope with a slight deviation from a value of 1 (Figure 19). From these observations it is not clear whether the 10% increase should be considered significant. However, more importantly, is that the addition of CO_2 did not result in a significant decrease in T_{exc}, which would seem to indicate a decrease in plasma energy.

Electron Number Density

Since a possible candidate for analyte excitation in a He plasma is the free electron, the electron number density (ne^-) is thought to be an important parameter in evaluating the energy state of a He MIP. The utility of this measurement has been demonstrated with Ar microwave induced plasmas where the introduction of 100 atm of CO_2 decreased the n_e^- by a factor of 10 [38] from the pure Ar plasma. The n_e^- in this study was determined by spectrometric measurement of the Stark broadening of the Hβ line at 486.15 nm [48]. The

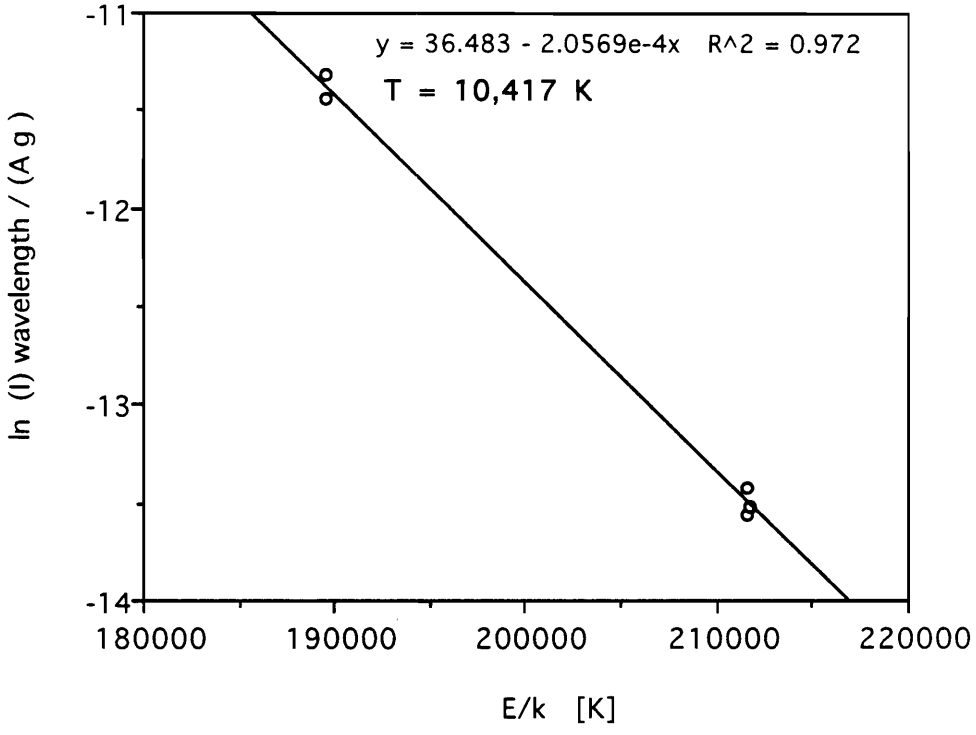

Figure 17: Boltzmann Plot of Cl Line Intensities for the Pure He MIP.

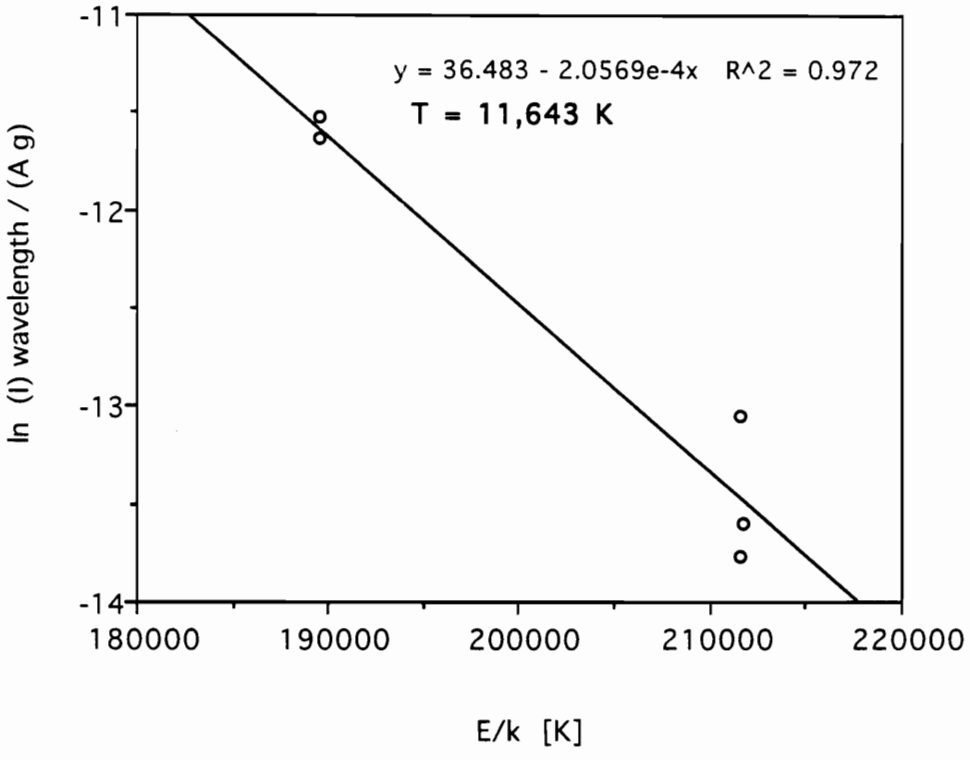

Figure 18: Boltzmann Plot of Cl Line Intensities for the He/CO_2 MIP.

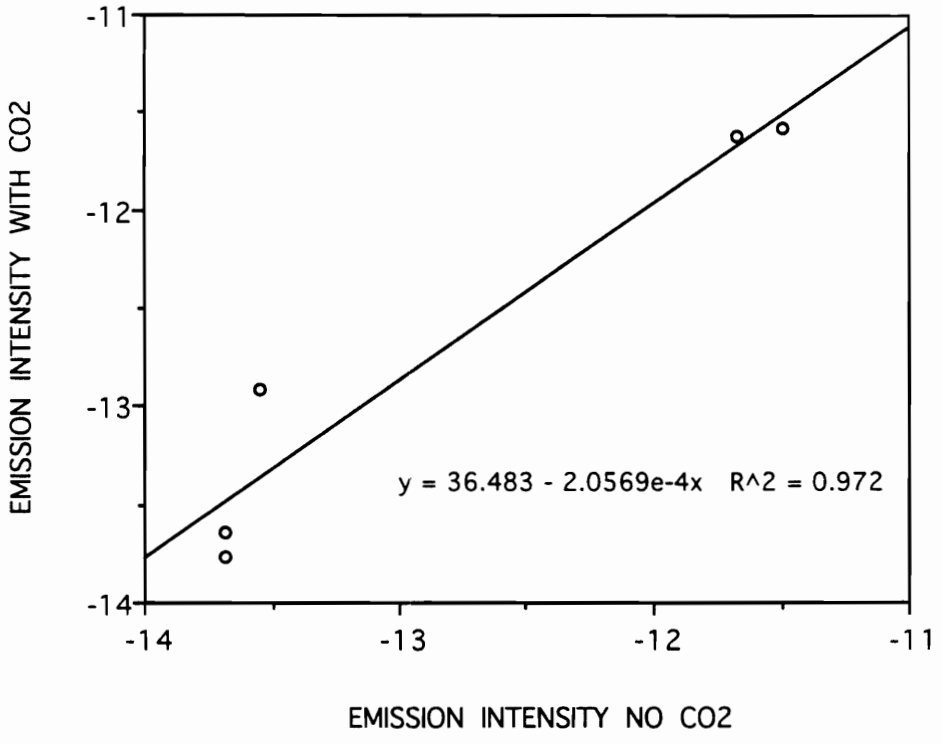

Figure 19: Slope Comparison of Cl Line Intensities for He and He/CO_2 MIP.

addition of 100 atm of CO_2 to a 150W He plasma resulted in no detectable effect on the density of electrons present in the discharge. The n_{e^-} value remained relatively constant, at roughly 1 X 10^{15} e^-/cc. This observation seems to indicate that the energy of each plasmas, with respect to the number of free electrons, is constant.

Ionization Temperature

Cd and Ca

The ionization temperature of a He plasma may be determined with a variety of probe species, most of which are metals. It was thought necessary to select only two metal probes which have some difference in excitation energy (Table 5). Cd and Ca were selected as the species to represent T_{ion} of the two plasmas. The relative intensities of the Cd 226.5 nm ion and 228.8 nm atom line, along with T_{exc}, electron number density, and appropriate spectroscopic constants, were entered into a Basic computer program which calculates T_{ion} using an iterative process. The same calculation was performed with the intensities of the Ca 422.7 nm atomic line and the 396.8 nm ion line The introduction of CO_2 into a He MIP yielded results much like those obtained with T_{exc}: a slight increase in T_{ion} was observed with both spectrometric species (Table 7). However, due to the 3% error associated with these calculations the change is not significant. Again, it is important to note that there was no significant decrease in T_{ion}, as would seem to be indicative of a less energetic plasma.

Rotational Temperature

With all other conventional diagnostic measurements indicating no significant effect of CO_2 on a He plasma, it was necessary to employ rotational temperature measurements in our investigations. Rotational temperature measurements have been carried out on a variety of analytical plasma types in addition to flames. The two most common species monitored

for rotational spectra are the OH radical and the N_2^+ molecular ion [49-53]. For a more detailed description of these temperature determinations the reader is directed to a study performed by Caruso *et al.*[52] which provides a direct comparison of measurements obtained with each of these two rotational species.

OH

Measurement of a [$A^2\Sigma^+ - X^2\Pi_i$] transition, Q_1 branch of the OH radical rotational spectrum (306 - 314 nm) was performed according to references 51 and 54. The spectrometric constants utilized in this calculation are listed in Table 8. While measurement of the OH rotational spectrum was accomplished with the pure He plasma, the addition of 100 atm (0.7%) CO_2 resulted in a severely attenuated signal, which prevented accurate measurement of T_{rot} in either the axial or radial viewing mode (Figure 20). These results are contrary to those of Mermet *et al.* [49] who successfully measured T_{rot} using OH in He and He/CO_2 plasmas generated with a surfatron device. The ability of the surfatron system to generate measurable OH rotational spectra with the addition of CO_2 is thought to be a factor of the reduced pressure conditions under which the surfatron plasma is operated. At pressures less than a few hundred atmospheres the OH species encounter fewer destructive collisions. As a consequence, the OH are longer lived species which can be measured readily. The increased rotational temperatures observed by Mermet *et al.* with the addition of CO_2 suggests that the gas kinetic temperature of the plasma is increasing with added mobile phase. With higher plasma kinetic temperatures it is implied that the analyte exciting ability of the He/CO_2 plasma would be higher than the pure He plasma. However, the diminished analyte emission that results from the addition of this foreign gas suggests that the CO_2 plasma species may be shortening the lifetime of the excited OH molecule by

Table 8:

Spectrometric Constants of OH used in Rotational Temperature Determinations

K	λ (nm)	E_{exc} (cm^{-1})	A (10^8 s^{-1})
1	307.844	32475	10.0
2	307.995	32543	17.0
4	308.328	32779	33.7
5	308.520	32948	42.2
6	308.734	33150	50.6
8	309.239	33652	67.5
9	309.534	33952	75.8
10	309.859	34283	84.1
13	311.022	35462	100.6
14	311.477	35915	108.8
15	311.967	36397	125.2
16	312.493	36906	133.3
17	313.057	37444	141.5
18	313.689	38008	149.6
19	314.301	38598	157.7

E_{exc} = excitation energies

A = rotational transition probabilities

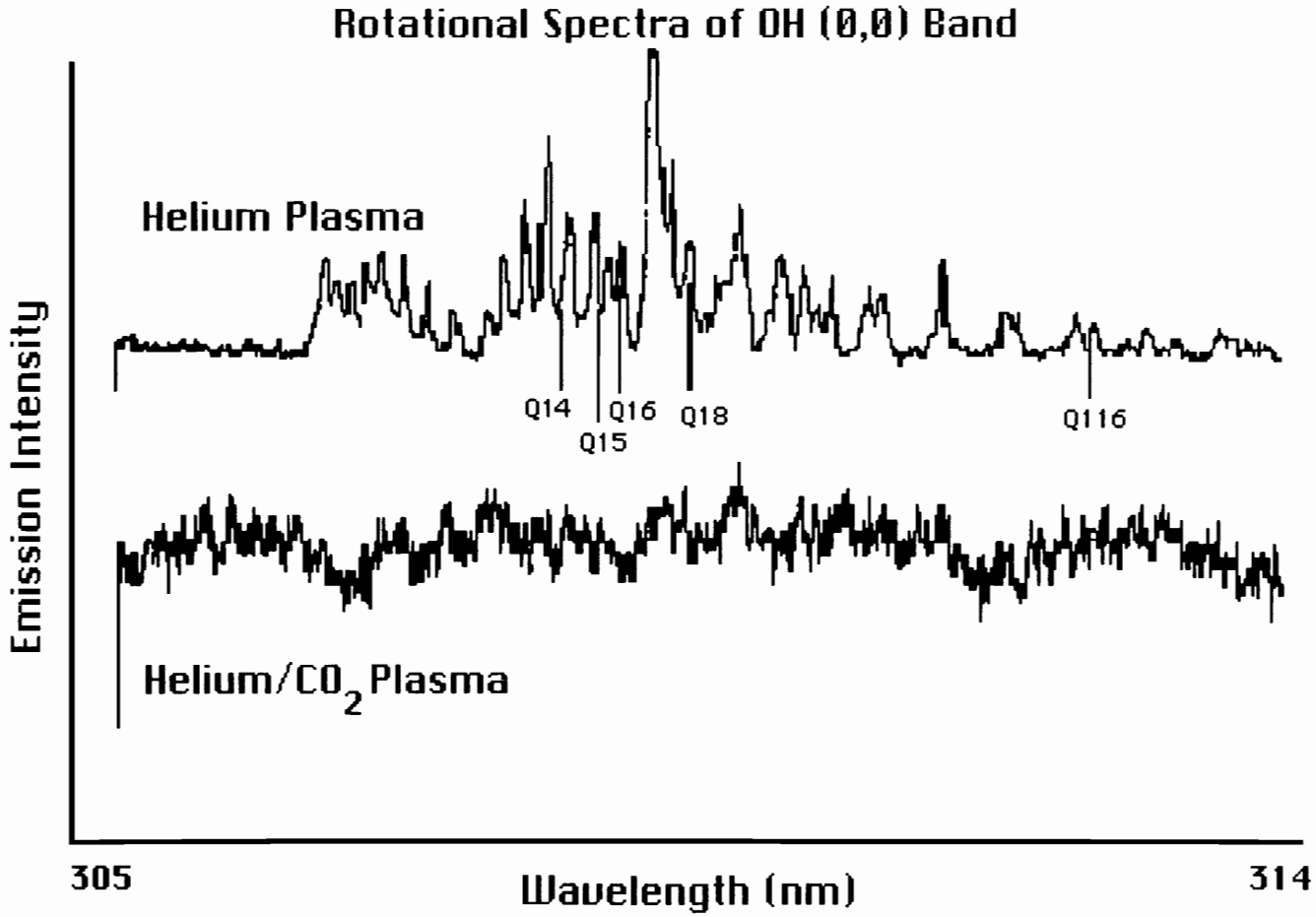

Figure 20: Rotational Spectra of OH band with and without CO_2

quenching. Alternatively, the result of the introduction of CO_2 may be generating a lesser degree of analyte fragmentation relative to the He^+ species, leading to reduced analyte emission intensity.

N_2^+

Successful measurement of the rotational spectra produced by N_2^+ species in pure He MIPs has been demonstrated [50-52]. An attempt was made in this investigation at measuring the rotational temperature of the plasmas by monitoring the N_2^+ [$B^2\Sigma_u^+$-$X^2\Sigma_g^+$ (0,0)] "1st negative system" present in the 388.0 - 391.5 nm region [51]. It was necessary to dope the He plasma with 10 mL/min of analytical grade N_2 in order to generate rotational spectra of adequate intensity. Measurement of the N_2^+ rotational spectra was accomplished with the pure He plasma. However, spectral interference due to CN molecular band emission prevented unambiguous measurement of the N_2^+ rotational bands with the CO_2-doped He plasma (Figure 21). Measurement of this temperature for the He/CO_2 plasma was also attempted in the radial mode with no enhancement of the rotational signal. The spectrometric constants used in these calculations are listed in Table 9.

Failure of LTE-based Diagnostic Measurements

Thus far we have exhausted the possibilities of monitoring the energetic state of a He MIP with the introduction of CO_2 using conventional spectroscopic techniques. It was believed that at least one of the conventional diagnostic methods employed in this study would shed some light on the changing excitation conditions of the He MIP with addition of a foreign gas. However, measurement of different spectrometric species in the temperature determinations has not provided any indication of a change in the excitation properties of the plasmas studied. As a result, a closer look needs to be taken at the

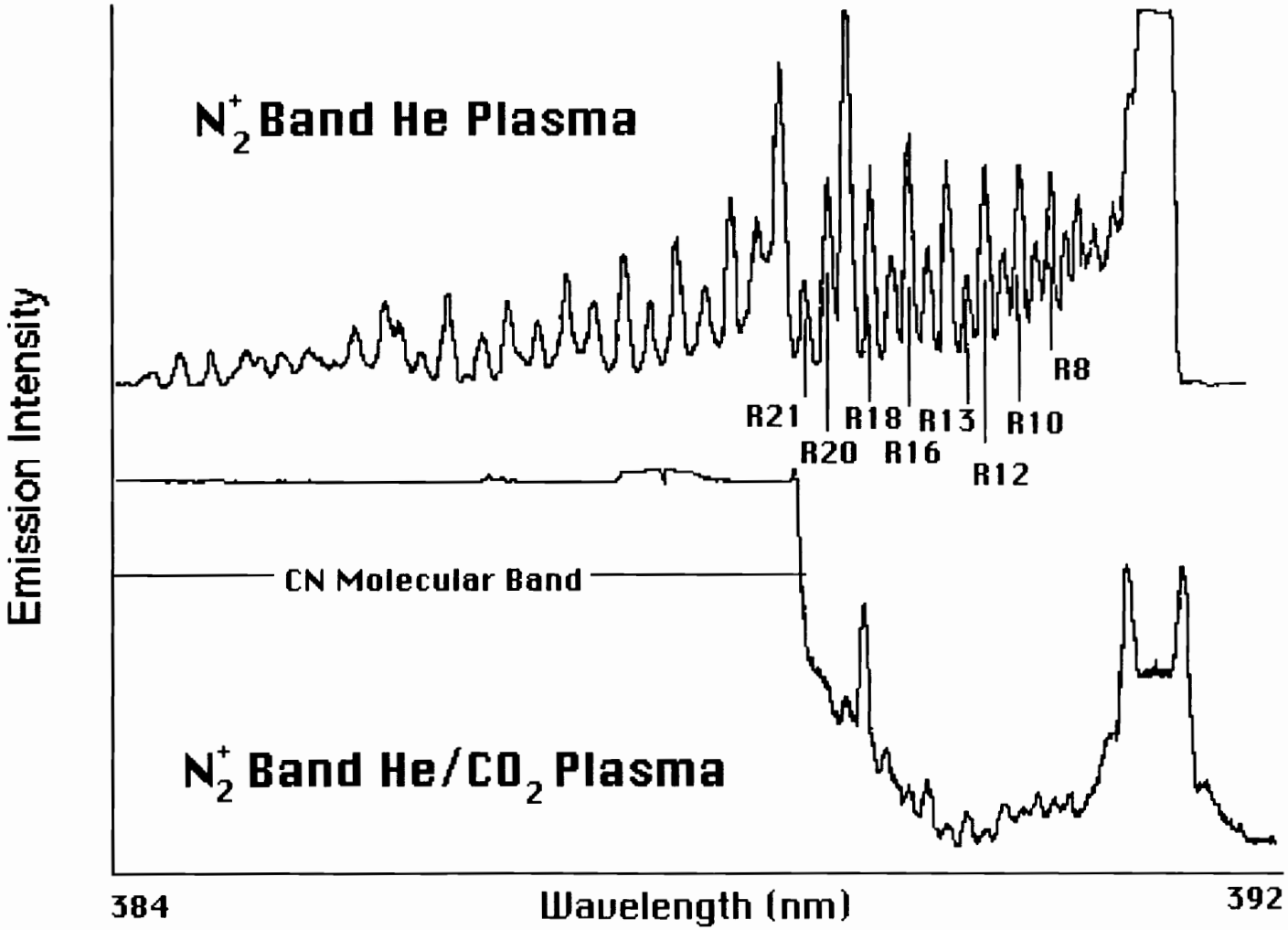

Figure 21: Rotational Spectra of N_2^+ Band with and without CO_2

Table 9:

Spectrometric Constants of N_2^+ Used in Rotational Temperature Determinations

K	λ (nm)	(K" + 1) (K" + 2)
6	390.49	56
7	390.40	72
8	390.29	90
9	390.19	110
10	390.08	132
11	389.97	156
12	389.85	182
13	389.73	210
16	389.33	306
18	389.04	380
20	388.74	462
21	388.58	506

K = quantum number

underlying relationships upon which each of these calculations is based and at the existence of a state of local thermodynamic equilibrium. Subsequent paragraphs will discuss the apparent failure of each of these diagnostic methods at accurately representing the energetics of a He MIP.

Excitation Temperature

Accurate determinations of T_{exc} in a plasma is dependent upon the establishment of a state of LTE. In order for LTE to exist in any environment local Maxwell, Saha, and Boltzmann equilibria must be obeyed. It can be seen from the Boltzmann plots of He and Cl (Figures 14,17) that a linear relationship exists. This is an indication that Boltzmann equilibria are in fact being obeyed by the spectrometric species in each of the plasmas. With this criterion being met, a calculation of T_{exc} from the relative intensity measurements of the selected species should be readily achieved. In considering the Boltzmann relation used to calculate T_{exc} (Chapter 3), the only variables between the pure He plasma and the He/CO_2 plasma are the relative intensities resulting from the selected atomic transitions. Following this Boltzmann equation, the only way for two different plasmas to yield the same T_{exc} is if the relative intensities of the emissions were affected to the same degree. We have demonstrated in Chapter 4 that transitions of different energies are affected to different degrees with the introduction of CO_2. Therefore, these measurements using the Boltzmann relationship cannot be used to predict the relative changes in emission intensity and, as a result, cannot be used to evaluate the energetics of He/CO_2 plasmas.

Electron Number Density

The density of electrons in the He and He/CO_2 plasmas investigated in this study has been shown to be roughly the same. While n_{e^-} is not dependent on the existence of

LTE, its lack of sensitivity to changing plasma conditions will be discussed. It was suspected that the introduction of CO_2 into the He MIP would result in a decrease in the number of free electrons which, in a pure He plasma, are stripped from the He atom to produce He^+ species. A possible explanation for the unchanging n_e^- is the existence of an equilibrium that is established between the neutral plasma species (CO_2 and He) and the charged plasma species (i.e. electrons) similar to that found in flames. If this theoretical equilibria is obeyed the introduction of CO_2 simply provides an additional neutral from which electrons can be stripped, resulting in a free electron concentration which ultimately remains the same. The lower ionization potential of CO_2 (13.77 eV) relative to He (24.56 eV) should result in a higher number of electrons being taken from the CO_2 molecule, resulting in a decrease in the relative He^+ concentration.

Ionization Temperature

The ionization temperature of a plasma can be determined with the use of the Saha-Eggert relation:

$$(I_i/I_a) = [4.83 \text{ X } 10^{15}/n_{e-}] (g_pA_{pq}/\gamma)_i(\gamma/g_pA_{pq})_a \text{ x } T^{3/2} * \exp[(-E_i - E_{pi} + E_{pa}) / kT$$

Considering observation of a constant electron density and T_{exc} between the He and He/CO_2 plasmas, the only variable which could allow a distinction between the energetics of each of the plasmas is the relative intensity of the selected atomic and ionic spectrometric species. As with T_{exc}, if the condition exists where the observed transitions are affected to the same degree then no significant change in plasma ionization temperature will be detected. Again, is has been demonstrated that different electronic transitions are affected to different degrees in the presence of CO_2, especially in comparing atomic vs. ionic states.

Thus, it seems apparent that the Saha-Eggert relation, as with the Boltzmann equation, is not sensitive enough to be used for temperature determinations in a CO_2-doped He MIP.

Rotational Temperature

In the case of N_2^+, its rotational spectra was masked by the CN molecular band, resulting in an indeterminate rotational temperature of the He/CO_2 plasma. While this determination did not provide for a temperature comparison between the two plasmas, the Boltzmann plots of the data obtained in the pure He plasma did give an indication that the N_2^+ rotational species follow a Boltzmann distribution (Figure 22). Considering the failure of the other diagnostic measurements, it does not seem likely that an interference free N_2^+ spectra in the He/CO_2 plasma would have resulted in significant difference in T_{rot} relative to the He plasma.

Measurement of the OH rotational temperature also resulted in an indeterminate temperature of the He/CO_2 plasma. However, examination of the Boltzmann plot obtained with the He plasma (Figure 23) seems to indicate that the OH species obey Boltzmann equilibria. Since a similar measurement of OH_{rot} has been successfully performed on a reduced pressure He MIP [49], it is important to consider the results obtained in these investigations. Because the introduction of CO_2 into this reduced pressure system resulted in a slight increase in T_{rot}, indicating an increase in energy of the plasma, it is likely that interference free results in an atmospheric pressure He MIP would reveal the same conclusion: that T_{rot} determination with the OH species is not representative of the energetics of a He/CO_2 plasma. Whatever the cause of the apparent insensitivity of these diagnostic calculations to the introduction of CO_2 to a He plasma, the end result is a distribution of plasma species and associated internal, translational, rotational, and

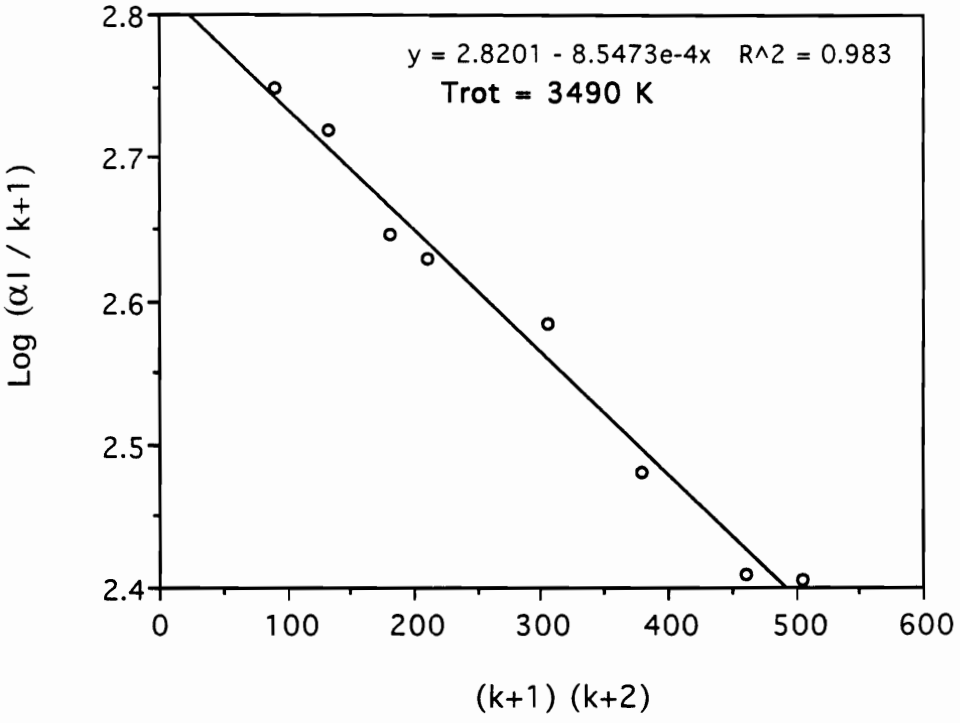

Figure 22: Boltzmann Plot of N_2^+ Line Intensities for the Pure He MIP.

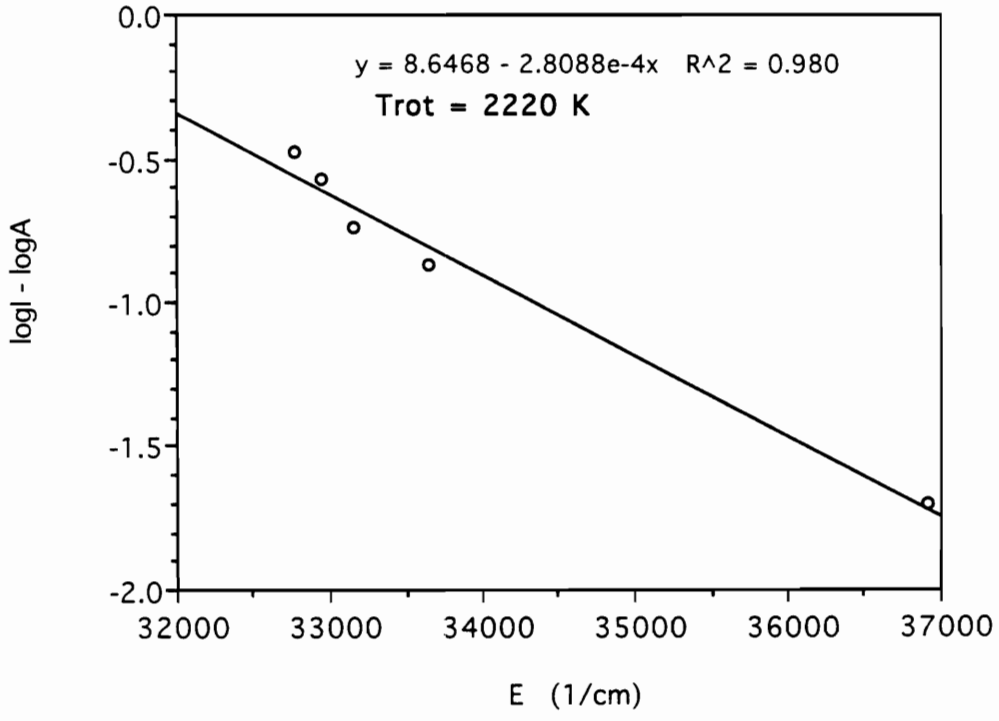

Figure 23: Boltzmann Plot of OH Line Intensities for the Pure He MIP.

vibrational energies, which maintains a relatively constant value (± 5%) for T_{exc}, T_{ion}, and T_{rot} but, which is not in a form that allows efficient transfer to non-metal species. It is likely that the CO_2 plasma species are not of sufficient energy to effectively populate many non-metal energy levels, whereas the He^+ species, possessing 24.56 eV, are of sufficient energy.

Charge Transfer Theory

The failure of conventional LTE- based diagnostics to describe the redistribution of plasma energy with the introduction of supercritical CO_2 into a He MIP has led to examination of other plasma processes and theories, ones which may provide insight to the response of a He MIP to CO_2. One such theory that has been developed recently by Carnahan, Hieftje, and Jones is based upon charge transfer [55,56]. Basic charge transfer theory predicts that an energy match between the moving particle and the transition energy of the colliding partner will result in a transfer of charge between the two species upon an inelastic collision and thus, a change in internal energies of both particles. Basic CTT also states that the closer the energy match (small energy defect) the higher the probability that a transfer of charge will take place upon collision.

The charge transfer theory discussed here considers the basic requirements for CT to take place and relates the energies of plasma species present in He discharges to transition energies required for analyte excitation. It has been shown that a variety of reactive species exist in a He plasma including; free electrons, ground state He atoms, excited He atoms, He ions, excited He ions, excited diatomic He , and diatomic He ions [55]. Through several investigations involving detailed evaluations of the energies possessed by each of the plasma species, a charge transfer initiator thought responsible for a majority of non-metal analyte excitation was singled out. The first charge transfer model presented was

based upon specific electronic transitions of Cl. The single step process considered to be responsible for a majority of energy transfer between the plasma and Cl is as follows:

$$Cl(0eV) + He^{+}(24.56eV) \rightarrow Cl^{+*}(24.59eV) + He(0eV)$$

This reaction demonstrates the small energy defect (0.03 eV) between the energy of the singly ionized helium species (He^{+}) and the energy required to promote the Cl atom from ground state to the $3s3p^5\ ^3P^0$ excited ionic state. Although this transfer scheme would seem to only be responsible for promoting one particular transition, it is actually the initiator for many other nonmetal transitions. Thermal excitation is thought to be responsible for populating energy levels above the already achieved charge transfer induced excited state. It was also found that those Cl transitions demanding < 7 eV beyond this excited state are readily observed in the He MIP [45]. Those transitions which do not involve achieving the $3s3p^5\ ^3P^0$ state, or require >7 eV above this state are not observed in the He plasma. Similar charge transfer relationships have been established between the He ion and other non-metals such as S, P, Br, and I [56].

Depletion of He^{+}- Kinetic Considerations

In considering the CTT and the role of He^{+} in non-metal excitation, it follows that the decrease in analyte emission observed in the presence of CO_2, or other molecular gases [57,58], is a result of the decrease in the concentration of He^{+}. Decrease of the He^{+} species has been documented with the introduction of air into a He MIP [58]. This investigation involved monitoring the relative He^{+} concentration using mass spectrometry. An attempt was made in the current investigation to monitor the relative He^{+}concentration with the introduction of CO_2 by observing the 656.0 nm helium ion line (Figure 24). These

results show that the relative population of the He^+ state is decreasing in the presence of this mobile phase.

While the charge transfer theory provides much insight to the analyte excitation processes occurring in a 150W He MIP and their response to CO_2, it does not provide any detailed information about the actual mechanisms involved in the reduction of the He^+ species. A literature search of kinetic studies performed in He discharges has revealed several critical relationships which seem to support the charge transfer theory in addition to supplying detailed information on specific plasma processes. In considering the possibility that the He metastable atom is responsible for generating a significant portion of the total He^+ population through the reaction:

$$He(2^3S) + He(2^3S) \rightarrow He^+ + He \quad (1),$$

It follows that a plasma perturbation which decreases the concentration of metastable He atoms will also result in a decrease of He^+ species. Lee and Collins have determined the rate of destruction of the He metastable species in high pressure He afterglow discharges brought about by the introduction of the reactant gases Ne, Ar, N_2, CO, CO_2, and CH_4 [59]. The results of this comparative study indicate that the destruction frequency of the He metastable atom is significantly larger in the presence of CO_2 than with any of the other gases studied. A second-order bimolecular reaction that demonstrates a possible destruction mechanism of He metastable species when encountering a reactant gas molecule is as follows:

$$He(2^3S) + X \rightarrow He + X^+ + e^- \quad (2)$$

Here, X represents a reactant gas, in this case CO_2. If the critical He ion concentration is dependent on the abundance of $He(2^3S)$ it seems feasible that the occurrence of reactions

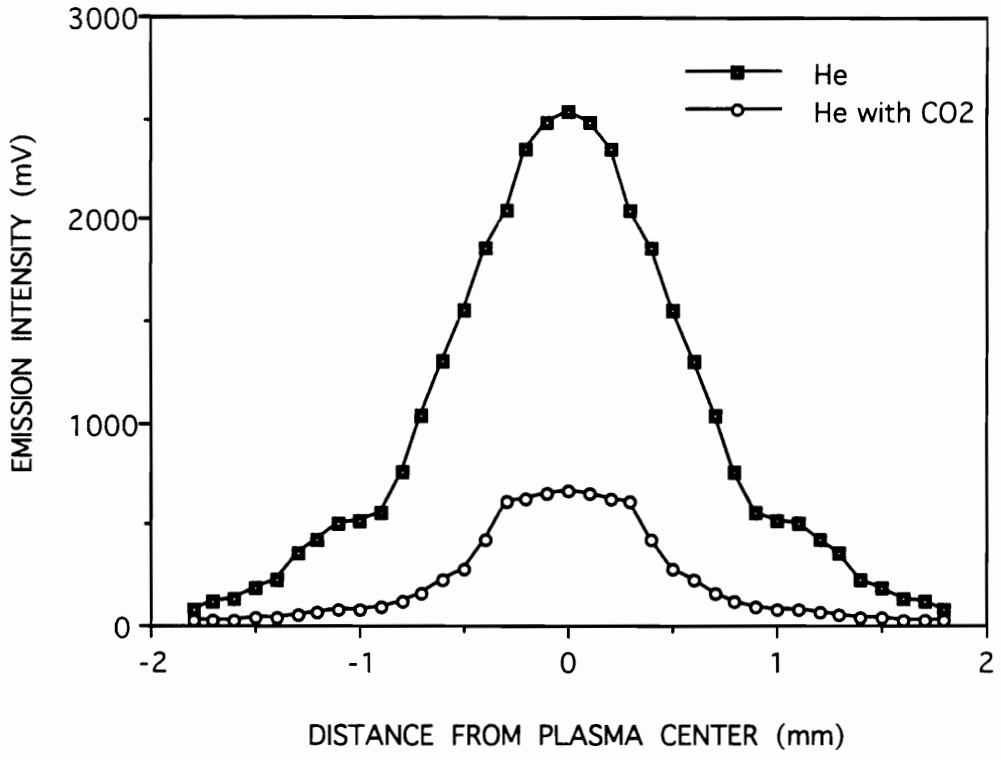

Figure 24: Axial Scan of He^+ Emission at 656.0 nm

1&2 is ultimately responsible for the decreased population of He^+ and consequential decrease in analyte emission intensity observed in He/CO_2 microwave plasmas.

SUMMARY

The inability of conventional diagnostic measurements to accurately describe the excitation properties of a low powered He MIP with the introduction of supercritical CO_2 has been demonstrated, although the reason(s) for their inadequacy is not clear. The redistribution of plasma energy, and consequential decrease in excitation ability, that occurs when CO_2 is present in a He discharge is manifested solely through the depression of the analyte emissions themselves. Adoption of the charge transfer theory developed by Carnahan *et al.* has proved critical in the understanding of analyte excitation and specifically the role of the He^+ species in the excitation of nonmetals. Examination of kinetic studies performed by Collins and Lee has provided reasonable mechanisms by which the depletion of He^+ is occurring. The combination of CTT and kinetic data described in this study has allowed for the modeling of a logical detailed pathway for describing the effect of supercritical CO_2 on the He MIP.

Chapter 6

STUDIES ON SUPERCRITICAL FLUID EXTRACTION-MICROWAVE INDUCED PLASMA ATOMIC EMISSION SPECTROMETRY

As Chapters 4 and 5 describe our efforts in determining the effect of supercritical CO_2 on the He MIP, this chapter considers a similar sample introduction technique into an Ar MIP utilizing supercritical fluid extraction with CO_2. The success of supercritical CO_2 as an extracting medium for a variety of sample types and matrices is discussed in the introduction. The different chromatographic methods and detectors used to further separate and detect components as they exit the SFE system have also been described. This chapter will describe an interface between a supercritical fluid extraction system and a plasma-based detector without the use of an intermediate chromatographic separation. While these initial studies do not involve determination of diagnostic parameters, as in the two previous chapters, it does describe the response of the Ar MIP iron with the introduction of relatively high flows of CO_2. These studies demonstrate the feasibility of direct detection of SFE extracts utilizing element specific detection plasma atomic emission spectrometry.

RESULTS AND DISCUSSION

Plasma Stability

The introduction of analyte from the SFE system to the MIP is similar to the introduction of analyte to the plasma via SFC. However, when performing SFC studies the mobile phase (CO_2) enters the plasma before the analyte. This condition allows tuning of the cavity to accommodate the presence of the CO_2 flow before detection of the analyte. It also provides the plasma with a chance to restabelize prior to analyte detection. Introducing samples to a plasma with the SFE system described in this section creates a different situation. In this case, the CO_2 and analyte enter the plasma simultaneously as the outlet of

the syringe pump is opened. This presents the plasma with a sudden burst of molecular gas at the time of analyte detection. Thus, a major concern of this procedure was the stability of the Ar discharge during monitoring of the analyte emission. Extractions of ferocene spiked in sea sand were carried out at various CO_2 pressures ranging from 100-400 atm. In each case the plasma was neither extinguished nor destabilized with an Ar flow rate of 2.5 L/min.

Difficulties with the Interface

Several interesting, yet undesirable, effects were noted to occur with this interface which required minor modification of the system to be overcome. An occasional problem encountered with SFC and SFE is partial or complete plugging of the outlet restrictor. The existence of subcritical fluid conditions at the end of the restrictor result in a decreased solvating ability of the mobile phase and, thus, a deposition of analyte in the restrictor tip. This phenomena has been shown to be dependent on sample type, restrictor type, size, and temperature, as well as mobile phase composition.[18,60-64] Deposition of ferrocene was observed to occur in the restrictor end while performing extractions with an analyte concentration of 0.8 mg/mL. Partial and/or complete plugging of the restrictor resulted with both the 25 μm and 50 μm linear restrictors. Partial plugging was evident as successive extractions of analyte at the same concentration yielded smaller signals until complete plugging was experienced. Removal of 1 cm of fused silica from the end of the restrictor resulted also in plug removal without altering the extraction conditions. It is important to note that linear pressure restrictors are particularly susceptible to pressure gradients near the restrictor tip. It is suspected that the use of integral, tapered, or other restrictor designs might prove less troublesome in these types of analyses.

An additional problem observed in these studies was the deposition of analyte on the inner surface of the glass "T" into which the supercritical fluid and extract is introduced. Considering the smooth, clean inner surface of the "T", it seems unlikely that the analyte

would deposit here. Additionally, the orthogonal introduction of plasma gas, relative to the CO_2 flow, provides efficient plug free sample transfer to the plasma when employing SFC-MIP. Nonetheless, an occasional visible build up of analyte results if the SFE exit restrictor tip was positioned too close to the wall of the "T" (Figure 25). It is interesting to note that prior to the deposition of ferrocene was the formation of a light "frost" of solid CO_2 which might play a role in the attraction of analyte to the glass surface. Repositioning the restrictor tip to a greater distance from the "T" wall eliminated the problem of solute deposition. It is thought likely that heating the plasma gas prior to its point of intersection with the extract/CO_2 stream could lessen the degree of cooling caused by the rapidly expanding supercritical fluid, ultimately hindering solute deposition on the walls of the glass "T".

Effect of Extraction Pressure on System Performance

Complete dynamic extractions of ferrocene from the sea sand were accomplished at 100 atm of CO_2 pressure. The efficiency of extraction was determined as subsequent "blank" extractions yielded no Fe emission, as monitored by the 373.8 nm line. Extractions were carried out at 200, 250, 300, and 400 atm did not result in differences in peak height, peak width, or extraction time. This is not completely unexpected as the analyte is only adsorbed onto the silica surface and does not require an enhancement of solvent strength (higher density) to be removed. While employment of different extraction pressures did not result in physical changes in the extractograms achieved at each pressure it was necessary to increase the Ar gas flow lightly to accommodate the additional flow of CO_2 at extraction pressures above 300 atm. Even with the higher solvating power of CO_2 at higher pressures the restrictor still experienced plugging.

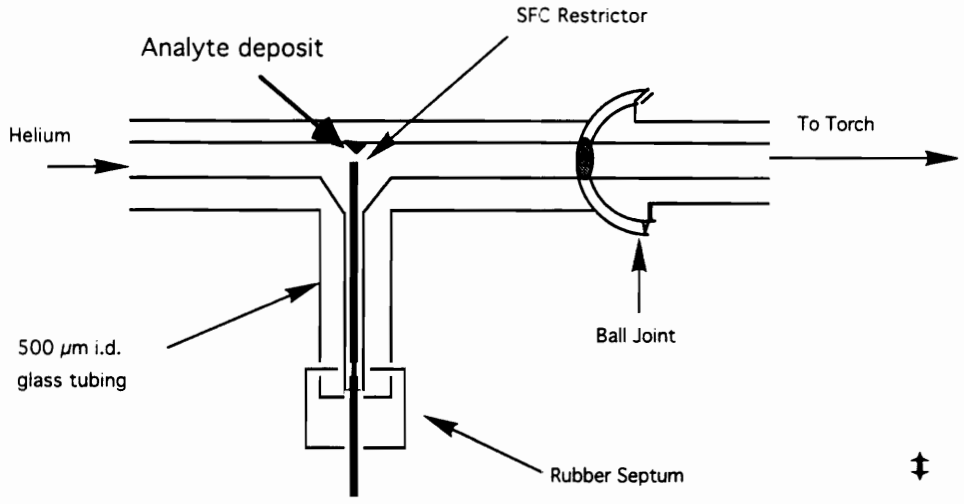

Figure 25: SFE-MIP Interface Demonstrating Analyte Deposition

Effect of Extraction Temperature on System Performance

The extraction temperature has been shown to have significant effects on the quality and speed of supercritical fluid extractions [65-67]. In order to study this effect on our system a range of temperatures from 40 -100°C was employed. As with the variable pressures, the different extraction temperatures resulted in no observable difference in extraction time, peak height, or width. Again, since the analyte is not strongly bound to the silica surface it is not suprising that changes in the solvating characteristics of the extractant (with temperature) do not effect the resulting extraction. Analysis of an analyte which is less soluble in supercritical CO_2 or which is incorporated in the sample matrix would most likely demonstrate significant changes in extraction characteristics with different extraction pressures and temperatures. However, it is not the purpose of this preliminary study, nor would it be appropriate, to evaluate an unoptimized SFE-MIP system with complex real-world samples.

Linearity of SFE-MIP

An important parameter in evaluating the performance of a detector is the range of concentrations of sample that yield a linear response with peak area (or height). Extractions of ferrocene in this study were carried out at concentrations of 0.25 to 1.0 mg/mL. The response of the Ar MIP to these concentrations of ferrocene is represented in Figures 26 and 27. Each data point in the latter figure is the average peak area of 4 replicate extractions which were all carried out at 225 atm of CO_2. The figure does not include the results achieved with 0.8 or 1.0 mg/mL ferrocene in CH_2Cl_2 due to the unavoidable restrictor plugging and consequential decrease in signal between successive extractions. As indicated in the figure the linearity of this technique includes a range of concentrations characteristic of a good portion of analyses of this type (0-100 µg ferrocene). It is important to note that

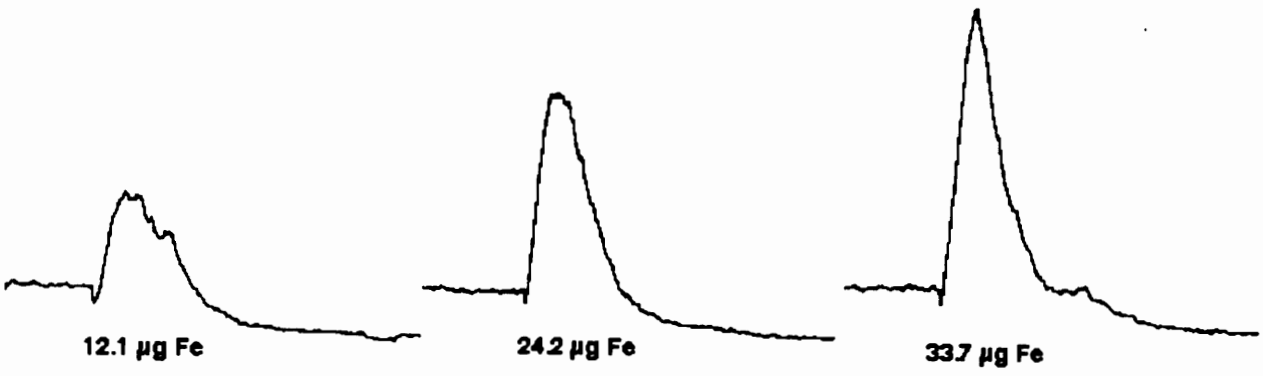

Figure 26: Detector Response of Ar MIP to Fe in Ferrocene Extracted with Supercritical CO_2

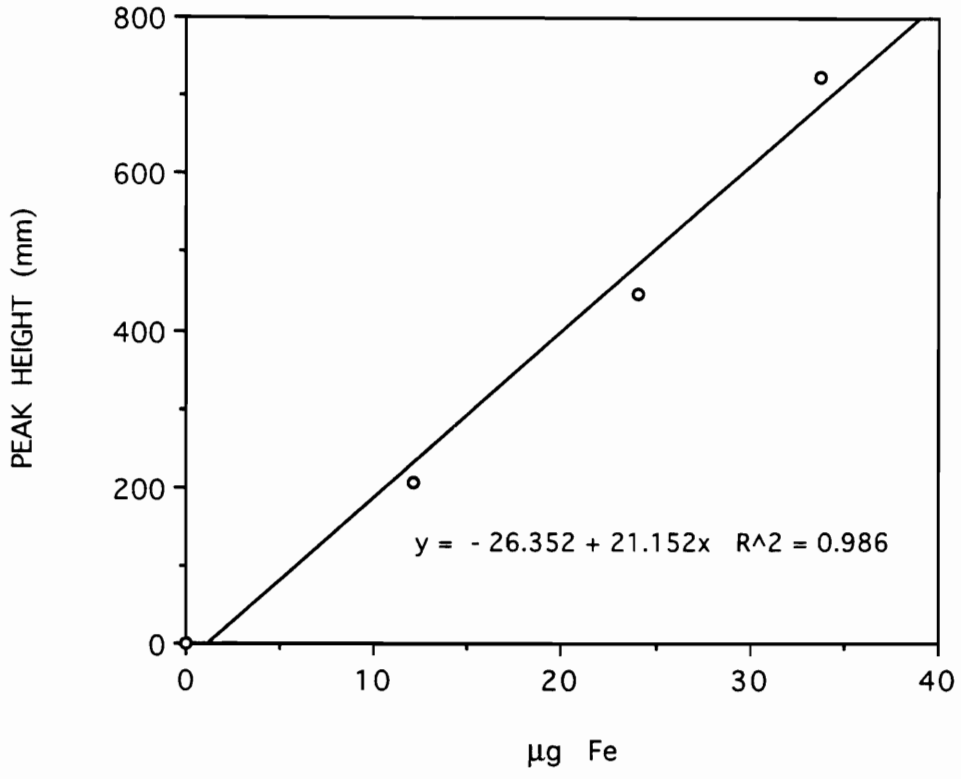

Figure 27: Calibration Plot of Fe Extracted From Sea Sand using SFE-MIP.

accurate determination of the pre-peak baseline was difficult to achieve since the plasma did not have time to completely stabilize following the introduction of CO_2 before the sample entered the plasma (Figure 26). As a result, the peak heights used to measure detector response were determined from the post-peak baseline, where the Ar/CO_2 plasma is stable. Measurement of peak area provided no further accuracy in representing the detector response due to the reasons just described. It is suspected that employment of an analyte that requires on the order of several minutes to extract would afford a more accurate, and more reproducible determination of the pre-peak baseline and peak parameters.

Repeatability

The relative standard deviation (RSD) of the ferrocene peak heights achieved by observation of the Fe 373.8 nm emission line are as follows: 80ppm Fe = 18% RSD, 160 ppm Fe = 16% RSD, and 225 ppm Fe= 14% RSD. While SFE/GC analyses have resulted in similar RSDs for certain compounds extracted from basil with an optimized system [61], it is believed that an increase in the number of replicates, better baseline determination, and the use of integral restrictors will allow much more reproducible results to be achieved with our system.

SUMMARY

The direct detection of supercritical fluid extract with an Ar MIP has been demonstrated. Element specific detection of Fe in ferrocene extracted from sea sand has yielded a linear response to concentrations ranging from 0-225 ppm Fe in CH_2Cl_2. The surge of supercritical CO_2 experienced by the Ar plasma by nature of the dynamic extraction has been shown not to extinguish or destabilize the Ar discharge even at pressures of 400 atm. While analyte deposition occurred inside the pressure restrictor and

on the inner surface of the glass "T" minor modifications of the interface allowed quantitative SFE-MIP to be achieved.

Chapter 7

CONCLUSIONS

A major objective of this work has been to provide a further understanding of the processes that occur in a low power He microwave induced plasma with respect to analyte excitation and energy perturbations resulting from the introduction of supercritical mobile phases via SFC. A second objective of this work, which developed as a consequence of the results obtained in carrying out the first objective, has been to critically evaluate plasma diagnostic measurements which have been used for 3 decades to describe the energetics of a variety of plasma types. The last major investigation of this dissertation was to examine the response of the MIP to the introduction of CO_2 via SFE.

While several research groups have reported the observation of a particular non-metal analyte transition being affected to a larger degree than another in a He plasma during the introduction of SFC mobile phase, no studies until this work describe a detailed study of this phenomena. Investigation of the emission signals of 5 non-metals has shown that the depression of analyte signal is not limited to a few select elements. Our findings indicate that their is no direct correlation between transition energy and degree of signal depression between elements. However, detailed examination of atomic and ionic emission lines of Cl has revealed the direct relationship between the energy required for a particular electronic transition and the degree to which the emission signal is depressed with the introduction of CO_2. This work has also demonstrated the importance of line selection in chromatography-MIP analyses. In the case of sulfur, if one were to perform analyses on the most intense ion line in the UV spectral region, the instability of this transition would lead to complications in quantitative determinations of SFC-MIP. On the other hand, if analyses were performed on the sulfur atom line in the IR, no complications with the introduction of the SFC mobile phase would arise. Thus, selecting emission lines for element selective

detection chromatography should not be based upon emission intensity only. Knowledge of the origin of the selected lines can provide useful information in predicting the response of any line to plasma perturbations.

Since interest in SFC-MIP has increased significantly in the last 5 years so have the number of publications in this area. A good number of these investigations have involved employing one or sometimes two diagnostic measurements, utilizing just one spectrometric species, in an attempt to monitor changes in energy of the plasma resulting from the introduction of the mobile phase. Until the work described in this dissertation, a direct comparison of the most "accurate" and, most commonly used, LTE-based diagnostic methods has not been attempted. The work described in this dissertation not only demonstrates that no one method is better than the rest at representing the energetics of a He MIP, but it has also revealed the limitations of these LTE-based methods when monitoring certain systems. Considering this particular aspect, it is believed to be misrepresentative when utilizing these diagnostic measurements to demonstrate the "robustness" or "stability" of a He MIP with the introduction of SFC mobile phases

The inability of conventional diagnostic methods to represent the energy changes in a He MIP with the introduction of CO_2 proves contradictory to previous reports which demonstate the success of these diagnostic measurements to describe the energy of an Ar MIP under similar conditions. This inconsistancy may be explained by the difference in excitation energy possessed by Ar and He plasmas, as this results in different mechanisms of analyte excitation in each discharge. Further studies involving a direct comparison of Ar and He MIPs with respect to reaction schemes affected by CO_2 could provide critical information in determining the limitations of LTE-based diagnostic measurements for different plasma types.

Speculations on analyte excitation processes in He discharges have been made since the early 1970's. Current debates still tackle the age-old controversy of which plasma

species are responsible for transferring energy to the analyte. Just recently, with the development of the charge transfer theory, credence has been given to the He^+ species as a major contributor to analyte excitation. Evidence of the mechanisms involving the He^+ species in the excitation of non-metals is strong. It is for this reason that this dissertation research incorporated this theory in describing plasma responses which, through other theories, could not readily be explained.

While the CTT provides useful insight to the excitation processes in a He MIP and offers a possible explanation for the decrease in emission intensity of nonmetals in the presence of CO_2, it does not consider other plasma processes that might directly connect the introduction of CO_2 to the decrease in He^+ species. A kinetic study performed in 1976 provides critical information about the interaction of a variety of plasma species with different doping gases in a He discharge. The conclusions of this study with respect to the role of the He metastable have seemed to fill the gap left by CTT in describing the observed signal depression phenomena. Simply put, it is the destruction of the He metastable, brought about by CO_2, that is responsible for the decrease in He^+ concentration and subsequent decrease in analyte emission observed in a He MIP. Piecing together the CTT and the kinetic data, it is our opinion that the critical plasma species and associated mechanisms that are responsible for the observed non-metal depressions have been revealed. Further kinetic studies could give additional support to the relationships described in this dissertation

Although it may seem that the use of a He MIP for detection of non-metal analytes in SFC is plagued by the introduction of mobile phase to the point where it may not be useful as a detector for SFC, excellent detection limits have been achieved by several research groups, even with the significant depression of analyte signal. Additionally, the He MIP has been shown not to be affected by the use of organic modifiers in SFC analyses

as so many other SFC detectors are[18]. This advantageous characteristic will be a large factor in further developments with SFC-MIP.

A relatively small section of this dissertation is devoted to the evaluation of the MIP as an element selective detector for SFE, as the investigations performed were of a preliminary nature and did not include complex samples or an optimization of the system. However, the potential of SFE-MIP for analysis of supercritical fluid extract without the need for a chromatographic step has been presented. Further studies employing the MIP as an element selective detector for SFE will involve the use of both Ar and He plasmas for determinations of metals and non-metals. Optimization procedures will also be carried out in order to demonstrate better the full potential of this technique for quantitative analyses of extracts removed from a variety of matrices.

References

1) L. Zhang and J. W. Carnahan, *Anal. Chem.* **63**, 212, (1991).

2) C. B. Motley and G. L. Long, *J. Anal. At. Spectrom.* **5**, 477, (1990).

3) J. Qinhan, F. Wang, C. Zhu, D. M. Chambers and G. M. Hieftje, *J. Anal. At. Spectrom.* **5,** 487, (1990).

4) L. J. Galante, M. Selby, D. R. Luffer, G. M. Hieftje and M. Novotny, *Anal. Chem.* **60**, 1370, (1988).

5) B. Riviere and J. M. Mermet, *J. Anal. At. Spectrom.* **3**, 551, (1988).

6) G. K. Webster and J. W. Carnahan, *Appl. Spectrosc.* **44,** 1020, (1990).

7) G. K. Webster and J. W. Carnahan, *Appl. Spectrosc.* **45**, 1285, (1991).

8) G. R. Ducatte and G. L. Long, submitted for publication *J. Anal. At. Spectrom.*

9) S. A. Estes, P. C. Uden, and R. M. Barnes, *Anal. Chem.* **53**, 1829 (1981).

10) J. Hubert, " Fundamental Studies on Surface Wave Induced Mixed Gas Plasmas," Presented at the Twentieth Annual Meeting of the Federation of Analytical Chemistry and Spectroscopy Societies, paper 636, October, (1993).

11) J. H. Kennedy, *Analytical Chemistry* . Saunders College Publishing, New York, (1990).

12) C. I. M. Beenakker, *Spectrochim. Acta,* **32B**, 173 (1977).

13) Matus, L. G., Boss, D. B., and Riddle, A. N., *Rev. Sci. Instrum,* **54**, 1667 (1983).

14) K. A. Forbes, E. E. Reszke, P. C. Uden and R. M. Barnes, *J. Anal. Atom. Spectrom.*, **6**, 57 (1991)

15) C. B. Motley, M. Ashraf-Khorassani and G. L. Long, *Appl. Spectrosc.* **43,** 737, (1989).

16) C. B. Motley and G. L. Long, *Appl. Spectrosc.* **44,** 667, (1990).

17) E. Klesper, A. H. Corwin, D. A. Turner, *J. Org. Chem.* **27**, 700 (1962).

18) M. L. Lee, and K. E. Markides, *Analytical Supercritical Fluid Charomatography and Extraction.* Chromatography Conferences, Inc., Provo, Utah, 1990.

19) J.M. Levy, R.A. Cavalier, T.N. Bosch, A.F. Rynaski, and W. E. Huhak, *J. Chromatogr. Sci.* **27**, 341 (1989).

20) H. H. Hill, Jr. and M. Morrissey, in *Modern Supercritical Fluid Chromatography,* C. M. White, Ed. Huethig, Heidelberg, 1988, P. 95

21) D. J. Bornhop, S. Schmidt, and N. L. Porter, *J. Chromatogr.* **459**, 193 (1988).

22) S. R. Weinberger and D. J. Bornhop, *J. Microcol. Sep.* **1,** 90 (1989).

23) R. Fuoco, S. L. Pentoney, and P. R. Griffiths, *Anal. Chem.* **61**, 2212 (1989).

24) K. H. Shafer, S. L. Pentoney, and P. R. Griffiths, *Anal. Chem.* **58**, 58 (1986).

25) D. R. Luffer and M. Novotny, *J. Chromatogr.* **517**, 477, (1990).

26) D. R. Luffer, L. J. Galante, A. D. Paul, M. Novotny and G. M. Hieftje, *Anal. Chem.* **60**, 1365, (1988).

27) Z. Liming, L. W. Carnahan, R. E. Winans, and P. H. Neil, *Anal. Chem.* **63,** 212, (1991).)

28) G. K. Webster and J. W. Carnahan, *Anal. Chem.* **64**, 50, (1992).

29) M. W. Blades, B. L. Coughlin, Z. H. Walker, and L. L. Burton, *Prog Analyt. Spectrosc.*, **10**, 57, (1987).

30) C. F. Baur, and R. D. Skogerboe, *Spectrochim. Acta* **38B** 1125-1134 (1983)

31) A. T. Zander, and B. M. Hieftje, *Applied Spect.* **35** 357, (1981).

32) D. C. Lorents, *Physica* **82C**, 19 (1976).

33) R. S. Van Dyck, Jr., c. E. Johnson and H. A. Shugart, *Phys. Rev.* **A 4,** 1327 (1971).

34) R. S. Van Dyck, Jr., C. E. Johnson and H. A. Shugart, *Phys. Rev.* **A 5,** 991 (1972).

35) N. E. Small-Warren and L. X. Chow Chiu, *Phys. Rev.* **A 11**, 1777 (1975).

36) B. W. Smith and M. C. Parsons *J. Chem. Educ.*, **50**, 679 (1973).

37) M. A. Wingerd, "A Multi-mode Spectrometer for Atomic Emission Spectrometry," Ph.D. Thesis, Virginia Polytechnic Institute and State University, (1990).

38) C. B. Motley, " The Evaluation of the High Efficiency Microwave Induced Plasma as an Elemental Selective Detector for Packed Column Supercritical Fluid Chromatography," Ph. D. Thesis, Virginia Polytechnic Institute and State University, (1989).

39) J. A. M Van Der Mullen, *Spectrochim. Acta,* **45** B, pp 1-13 (1990).

40) J. A. M. Van Der Mullen, *Spectrochim. Acta,* vol **44**B, 1067-1080, (1989).

41) N. W. Barnett and B. F. Kirkbright, *J. Anal. At. Spectros.*, **1**, 337 (1978).

42) H. R. Griem, "Spectral Line Broadening by Plasmas," Academic Press, New York,

(1974).

43) M. W. Blades, and B. L. Caughlin, *Spectrochim. Acta* **40B**, 579 (1985).

44) K. Tanabe, H. Haraguchi, and K. Fuwa, *Spectrochim. Acta.* **36B**, 119 (1981).

45) J. W. Carnahan, and G. M. Hieftje, *Spectrochim. Acta* **47B**, 731 (1992).

46) D. J. Jones and J. W. Carnahan, *Spectrochem. Acta* submitted 1992.

47) J.C. Miller, J. N. Miller, *Statistics For Analytical Chemistry* Ellis Horwood Limited, Chichester (1984).

48) D. J. Kalnicky, R. K. Kniseley, and V. A. Fassel, *Appl. Spectrosc.* **31**, 137, (1977).

49) B. Riviere, J. M. Mermet, and D. Deruaz, *J. Anal. At. Spectrom.* **3**, 551, (1988).

50) A. Besner, M. Moisan and, J. Hubert, *J. Anal. At. Spectrom.* **3**, 863, (1988).

51) M. H. Abdallah and J. M. Mermet, *Spectrochimica Acta,* **37B**, 391, (1982).

52) J. M. Workman, P. A. Fleitz, H. B. Fannin, J. A. Caruso, and C. J. Seliskar, *Appl. Spectrosc.* **42**, 96, (1988).

53) J. Cotrino, M. Saez, M. . Quintero, A. Menendez, E. Sanchez Uria, and A. Sonz Medel, *Spectrochimica Acta* **47B**, 425, (1992).

54) G. H. Dieke and H.M. Crosswhite, J. Quant. Spectrosc. Radiat. Transfer, **27**, 97, (1962).

55) J.W. Carnahan and G.M. Hieftje, *Spectrochimica Acta* **47B**, 731, (1992).

56) J. W. Carnahan, and K. J. Jones, *Spectrochimica Acta* Submitted 1992.

57) S. R. Koiryohann, *Anal. Chem.* **55**, 374, (1983).

58) D. M. Chambers, J. W. Carnahan, Q. Jin, and G. M. Hieftje, *Spectrochimica Acta.* **46B**, 1745, (1991).

59) F. W. Lee and C. B. Collins, *J. Chem. Phys.,* **65**, 5189, (1977).

60) B. W. Wright, and R. D. Smith, *Modern Supercritical fluid chromatography,* C. M. White, Ed. (Huethig, Heidelberg, 1988), p. 189.

61) J. C. Fjeldsted, R. C. Kong, and M. L. Lee, *J. Chromatogr.* **279**,449 (1983).

62) T. L. Chester, D. P. Innis, and G. D. Owens, *Anal. Chem.* **57**, 2243 (1985).

63) E. J. Guthrie and H. E. Schwartz, *J. Chromatogr. Sci.* **24**, 236 (1986).

64) B. E. Richter, *J. High Resolut. Chromatogr. Chromatogr. Commun.* **8**, 297 (1985).

65) J. W. King, *J. Chromatogr. Sci.* **27**, 355 (1989).

66) M. R. Anderson, J. T. Swanson, N. L. Porter, and B. E. Richter, *J. Chromatogr. Sci.* **27**, 371 (1989).

67) E. Stahl, K. W. Quarin, and D. Gerard. *Dense Gases for Extraction and Refining. Springer-Verlag, Berlin, 1988, p.87.*

68) K. A. McCleary, "Sample Introduction and Solvent Effects in an Argon and Helium Microwave Induced Plasma," Ph. D. Thesis, Virginia Polytechnic Institute and State University, (1992).

CURRICULUM VITAE

Gerald Roger Ducatte

Born:	August 16, 1966 Plattsburgh, NY
High School:	Northeastern Clinton Central Champlain, NY Diploma, June 1984
Undergraduate Education:	State University of New York Plattsburgh, NY Bachelor of Science, Chemistry, May 1988
Graduate Education:	Virginia Polytechnic Institute and State University Blacksburg, VA Doctor of Philosophy, Analytical Chemistry December, 1993
Dissertation:	Aspects of the Microwave Induced Plasma as an Element Selective Detector for Supercritical Fluid Chromatography and Supercritical Fluid Extraction Advisor: Dr. Gary L. Long
Professional Societies:	American Chemical Society

Publications

K. A. McCleary, G. R. Ducatte, D. H. Renfro and G.L. Long, "Evaluation of a Demountable Tangential Flow Torch for Microwave Induced Plasma Atomic Emission Spectrometry," Appl. Spectrosc. In press.

G. R. Ducatte, G. L. Long, "Effect of Chromatographic Gases on Non-metal Line Intensities in a Helium Microwave Induced Plasma," Appl. Spectrosc. In press.

G. R. Ducatte, E. D. Lancaster, and G. L. Long, "Element Specific Detection - Chromatography With Helium Microwave Induced Plasmas," invited review, submitted to Spectrochim. Acta., June 1993.

Manuscripts in Preparation

G. R. Ducatte, G. L. Long, "A Comparative Study of Diagnostic Methods for Determining the Effect of CO_2 on a Helium Microwave Induced Plasma," to be submitted to JAAS., November, 1993.

G. R. Ducatte, E. D. Lancaster, and G. L. Long, "On-Line Supercritical Fluid Extraction-Microwave Induced Plasma Atomic Emission Spectrometry," to be submitted to Anal. Chemistry, November, 1993.

Presentations

G. R. Ducatte, G. L. Long, "Effect of Chromatographic Gases on Non-metal Line Intensities in a Helium Microwave Induced Plasma," Nineteenth Annual Meeting of the Federation of Analytical Chemistry and Spectroscopy Societies, September 1992, Paper 439.

G. R. Ducatte, G. L. Long, "A Comparative Study of Diagnostic Methods for Determining the Effect of CO_2 on a Helium Microwave Induced Plasma," Twentieth Annual Meeting of the Federation of Analytical Chemistry and Spectroscopy Societies, October 1993, paper 148.

G. L. Long, G. R. Ducatte, E. D. Lancaster, K. A. McCleary, and L. D. Perkins, " Studies on Atomic and Molecular Gas Plasmas" Twentieth Annual Meeting of the Federation of Analytical Chemistry and Spectroscopy Societies, October, 1993, paper 638.